A highly immunogenic and protective MERS-Coronavirus vaccine based on recombinant MV vaccine platform

Anna H. Malczyk[a,b], Alexandra Kupke[c,d,*], Steffen Prüfer[a,*], Vivian A. Scheuplein[a], Stefan Hutzler[a], Dorothea Kreuz[e], Tim Beissert[f], Stefanie Bauer[e], Stefanie Hubich-Rau[g], Christiane Tondera[a], Hosam Shams Eldin[c,d], Jörg Schmidt[c,d], Júlia Vergara-Alert[c,d], Yasemin Süzer[a], Janna Seifried[a], Kay-Martin Hanschmann[h], Ulrich Kalinke[i,k], Susanne Herold[l], Ugur Sahin[f,g], Klaus Cichutek[a,b], Zoe Waibler[b,e], Markus Eickmann[c,d], Stephan Becker[c,d], and Michael D. Mühlebach[a,b,#]

Oncolytic Measles Viruses and Vaccine Vectors,[a] Novel Vaccination Strategies and Early Immune Responses,[e] Biostatistics,[h] Paul-Ehrlich-Institut, Paul-Ehrlich-Straße 51-59, Langen, Germany; German Center for Infection Research, Langen, Germany[b]; Institut für Virologie, Philipps Universität Marburg, Marburg, Germany[c]; Universities Gießen & Marburg Lung Center (UGMLC), Department of Internal Medicine II, Section of Infectious Diseases, Gießen, Germany[l]; German Center for Infection Research, Marburg, Germany[d]; TRON gGmbH, Mainz, Germany[f]; Universitätsmedizin Mainz, Mainz, Germany[g]; Institute for Experimental Infection Research, TWINCORE, Centre for Experimental and Clinical Infection Research, a joint venture between the Hannover Medical School and the Helmholtz Centre for Infection Research, Hannover, Germany[i]; German Center for Infection Research, Hannover, Germany[k]

[#]Address correspondence to Dr. Michael Mühlebach, Michael.Muehlebach@pei.de

[*]equally contributed

Running title: MV as vaccination platform against MERS-CoV

Word count abstract: 243 (abstract), 130 (importance)

Word count text: 8035

Abstract

In 2012, first cases of infection with the Middle East Respiratory Syndrome coronavirus (MERS-CoV) were identified. In the meantime more than one thousand cases of MERS-CoV infection have been confirmed, which typically are associated with considerable morbidity and, in approximately 30% of the cases, mortality. Currently, there is no protective vaccine available. Replication competent recombinant measles virus (MV) expressing foreign antigens constitutes a promising tool to induce protective immunity against respective pathogens. Therefore, we generated MVs expressing the spike glycoprotein of MERS-CoV in its full length (MERS-S) or a truncated, soluble variant of MERS-S (MERS-solS). The genes encoding for MERS-S and MERS-solS were cloned into vaccine strain MV_{vac2} genome and the respective viruses were rescued (MV_{vac2}-CoV-S and MV_{vac2}-CoV-solS). These recombinant MV were amplified and characterized in passages three and 10. The replication of MV_{vac2}-CoV-S in Vero cells turned out to be comparable with the control virus MV_{vac2}-GFP while titers of MV_{vac2}-CoV-solS were approx. 3-fold impaired. The genomic stability and expression of the inserted antigens was confirmed via sequencing of viral cDNA and immunoblot analysis. *In vivo*, immunization of $IFNAR^{-/-}$-CD46Ge mice with $2x10^5$ $TCID_{50}$ MV_{vac2}-CoV-S(H) or MV_{vac2}-CoV-solS(H) in a prime-boost regimen induced robust levels of both MV and MERS-CoV neutralizing antibodies. Additionally, induction of specific T cells could be demonstrated by T cell proliferation, antigen-specific T-cell cytotoxicity, and IFN-γ secretion after stimulation of splenocytes with MERS-CoV-S presented by murine DCs. MERS-CoV challenge experiments indicate protective capacity of these immune responses in vaccinated mice.

Importance

Although MERS-CoV has not yet acquired extensive distribution being mainly confined to the Arabic and Korean peninsulas, it could adapt to spread more readily amongst humans and thereby become pandemic. Therefore, the development of a vaccine is mandatory. The integration of antigen-coding genes into recombinant MV resulting in co-expression of MV and foreign antigens can efficiently be achieved. Thus, in combination with the excellent safety profile of the MV vaccine, recombinant MV seems to constitute an ideal vaccine platform. The present study shows that a recombinant MV expressing MERS-S was genetically stable and induced strong humoral and cellular immunity against MERS-CoV in vaccinated mice. Subsequent challenge experiments indicate protection of vaccinated animals, illustrating the potential of MV as vaccine platform with the potential to target emerging infections such as MERS-CoV.

Introduction

In November 2012, a novel coronavirus was identified for the first time in a patient from the Kingdom of Saudi-Arabia who displayed with severe respiratory disease and was treated in June 2012 in London, UK. Later this virus was termed Middle East Respiratory Syndrome-Coronavirus (MERS-CoV) (1). By December 26, 2014, 938 laboratory-confirmed cases of MERS-CoV mostly from the Kingdom of Saudi Arabia and neighboring countries were diagnosed, resulting in 343 casualties (2). Few cases of MERS-CoV were also detected in the USA, the UK, Netherlands, Austria, France, Greece, Italy, and Germany, indicating the viruses´ principle potential to spread (2). Fortunately, direct transmission upon contact with human patients seemed to be limited, yet, is still possible, as determined by analysis of household contact infections in MERS patients´ families (3) and as evidenced by a recent cluster of MERS infections in South Korea with 166 cases between May 20 and June 19 this year, including 106 third and 11 fourth-generation cases (4, 5). As a natural reservoir, dromedary camels have been identified as the most likely source, as indicated by partially identical genomes detected in viruses isolated from humans or camels (6, 7). Additionally, antibodies against the spike glycoprotein of MERS-CoV with virus neutralizing capacity were detected in camels (8–10) and infections of individuals with MERS-CoV have been reported after contact with infected camels (11, 12). Interestingly, while all other members of the C lineage of *Betacoronavirus* genus have been found in different bat species (13, 14), only closely related, most likely precursor viruses of MERS-CoV have been identified in *Neoromicia capensis* bats (15). Thus, MERS-CoV has zoonotic origin, but sustained infections, the severity of the disease, and the risk of virus adaption to gain efficient human-to-human transmission mandates the development of effective vaccines to combat local infections and to be prepared for the occurrence of eventually a global pandemic, as previously observed for SARS-CoV in 2003 (16).

Preceding the current MERS-CoV epidemic 10 years ago, SARS-CoV has been the first *betacoronavirus* arising from zoonotic origin with potential fatal outcome in human patients (1). Experimental vaccines protecting animal models against SARS have been developed (17–19), and the properties of such SARS vaccines may be applicable to vaccines that should protect against MERS-CoV infections. Both neutralizing antibodies and T cell responses are essential for prevention of SARS-CoV infection (17, 18). The Spike protein (S), a coronavirus class I fusion protein (20, 21), has been identified as the most immunogenic antigen of SARS-CoV inducing strong humoral as well as cellular immune responses (17, 19). Similarly, MERS-S expressed by recombinant modified vaccinia virus Ankara or recombinant adenoviral vectors have already been demonstrated to induce neutralizing antibodies (22, 23). The detected neutralizing capacity of induced antibodies is expected, since the receptor-binding domain (RBD) in the S1 domain of both SARS-CoV and MERS-CoV S proteins mediate host-cell receptor binding as pre-requisite for cell entry (24, 25). Thus, S1 is the main target of neutralizing antibodies (26). Also the RBD of MERS-CoV-S alone has been demonstrated to induce strong neutralizing antibody titers (23, 27–31). In combination with different adjuvants, even induction of T cell responses by the recombinant RBD has been described (31). Thus, a prototypic MERS-vaccine should base on MERS-S expression since the induction of neutralizing antibodies has been shown to be a direct correlate of protection in case of SARS-CoV (32) .

The measles vaccine is an efficient, live-attenuated, replicating virus inducing both humoral and cellular immune responses with an excellent safety record and probably life-long protection (33, 34). The vaccine´s manufacturing process is extremely well established (35) and millions of doses can be generated quite easily and quickly. Generation of recombinant measles virus (MV) from DNA via reverse genetics is feasible (35) and allows the insertion of additional transcription units (ATU) by duplication of sequences terminated by start and stop sequences (36). Hence,

genes expressing foreign antigens up to 6 kb can be cloned into MV backbone (36) eliciting co-expression of MV proteins and inserted genes. Besides marker genes (37) or immune modulators (38), expression of antigens from foreign pathogens like Hepatitis B or C virus (39, 40), HIV (41), West Nile virus (WNV) (42, 43), Dengue virus (44), Chikungunya virus (CHIKV) (45), or SARS-CoV (19) by recombinant MVs has already been demonstrated. Thereby, robust immune responses against vector and foreign antigens are induced after vaccination of transgenic, MV-susceptible IFNAR$^{-/-}$-CD46Ge mice (46) or non-human primates with respective recombinant MV, in general. Especially protection of vaccinated animals from lethal challenge with WNV (42) or CHIKV (45) was demonstrated indicating the high efficacy of the system. Interestingly, pre-vaccinated animals with protective immunity against measles were still amendable to vaccination with the recombinant MV, since significant immune responses against the foreign antigen(s) are consistently induced (41, 45), and the MV-based CHIKV vaccine demonstrated efficacy in phase I trials irrespective of measles immunity (47).

Here, we aimed at utilizing the efficacy of the MV vaccine platform by generating a live-attenuated vaccine against MERS-CoV based on recombinant MV$_{vac2}$. This recombinant virus reflects the MV vaccine strain Moraten (48), which is authorized for vaccination against measles. As antigen we choose the MERS-CoV S glycoprotein to induce neutralizing antibodies and robust cellular immunity. Two variants of the glycoprotein were analyzed as antigen: the full-length, membrane anchored MERS-S, and a truncated, soluble form lacking the transmembrane domain (MERS-solS). Both variants include the S1 domain as target structure. The soluble protein variant should be taken up better by B-cells (49–51), and thus should induce humoral immune responses more efficiently (52), potentially boosting virus neutralizing antibody titers (VNT). The respective genes were inserted into two different positions of the MV genome to modulate expression of the antigens, and all recombinant MV were successfully rescued. Cells

Journal of Virology

infected with such viruses expressed the desired antigens. Indeed, immunization of IFNAR$^{-/-}$-CD46Ge mice induced strong humoral and cellular immune responses directed against MV and MERS-CoV S, which were sufficient to protect vaccinated animals from MERS-CoV infection. Thereby, MV platform based vaccines are a powerful option to develop a pre-pandemic vaccine against MERS-CoV.

Material and Methods

Cells

Vero (African green monkey kidney) (ATCC CCL-81), 293T (ATCC CRL-3216), and EL4 mouse T (ATCC TIB-39) cell lines were purchased from ATCC (Manassas, VA, USA) and cultured in DMEM supplemented with 10% fetal bovine serum (FBS; Biochrom, Berlin, Germany) and 2 mM L-Gln (Biochrom). JAWSII dendritic cells (ATCC CRL-11904) were purchased from ATCC and cultured in MEM-α with ribonucleosides and deoxyribonucleosides (GIBCO BRL, Eggenstein, Germany) supplemented with 20% FBS, 2 mM L-Gln, 1 mM sodium pyruvate (Biochrom), and 5 ng/ml murine GM-CSF (Peprotech, Hamburg, Germany). DC2.4 and DC3.2 murine dendritic cell lines (53) were cultured in RPMI containing 10% FBS, 2 mM L-Gln, 1% non-essential aminoacids (Biochrom), 10 mM HEPES (pH 7,4), and 50 µM 2-Mercaptoethanol (Sigma-Aldrich, Steinheim, Germany). All cells were cultured at 37°C in a humidified atmosphere containing 6% CO_2 for a maximum of 6 months of culture after thawing of the original stock.

Plasmids

The codon-optimized gene encoding MERS-CoV-S (Genebank accession no. JX869059) flanked with *Aat*II/*Mlu*I binding sites in plasmid pMA-RQ-MERS-S was obtained by gene synthesis

(Invitrogen Life Technology, Regensburg, Germany). A truncated form of MERS-S lacking the transmembrane domain was amplified by PCR, flanked with *Aat*II/*Mlu*I binding sites, and fully sequenced. Both antigens, as well as the CMV promotor (54), were inserted into p(+)BR-MV_{vac2}-GFP(H) or p(+)MV_{vac2}-ATU(P) (48) via *Aat*II/*Mlu*I or *Sfi*I/*Sac*II, respectively, to generate p(+)PolII-MV_{vac2}-MERS-S(H), p(+)PolII-MV_{vac2}-MERS-S(P), p(+)PolII-MV_{vac2}-MERS-solS(H), or p(+)PolII-MV_{vac2}-MERS-solS(P). For construction of lentiviral transfervectors encoding the MERS-CoV antigens, the ORF of MERS-S was amplified by PCR with primers encompassing flanking *NheI/XhoI* restriction sites and template pMA-RQ-MERS-S. Details on primers and PCR are available upon request. PCR products were cloned into pCR2.1-TOPO (Invitrogen Life technologies) and fully sequenced. Intact antigen ORF was cloned into pCSCW2gluc-IRES-GFP (55) using *NheI/XhoI* restriction sites to yield pCSCW2-MERS-S-IRES-GFP.

Production of lentiviral vectors

Viral vectors were produced using 293T cells and polyethylenimine (PEI) (Sigma-Aldrich) transfection (56). $1x10^7$ 293T cells were seeded per 175 cm^2 cell culture flasks and cultured overnight. To produce VSV-G pseudotyped lentiviral vectors, these cells were transfected using a standard three plasmid lentiviral vector system. Cells were transfected with 17.5 µg pCSCW2-MERS-S-IRES-GFP transfer vector, 6.23 µg pMD2.G, and 11.27 µg pCMVΔR8.9 (57), as described (58). The medium was exchanged one day post transfection, and [$HIV_{MERS\text{-}S\text{-}IRES\text{-}GFP}$(VSV-G)] vector particles were harvested two and three days after transfection. For harvest of vector particles, the supernatant of three culture flasks was filtered (0.45 µm), pooled, and concentrated by centrifugation (100,000 × g, 3 h, 4°C). Pellets were resuspended in DMEM and stored at -80°C.

178 **Generation of antigen-expressing cell lines**

179 Syngeneic target cells based on the C57BL/6-derived DC lines JAWSII, DC2.4, DC3.2, as well
180 as T cell line EL-4 were transduced with [$HIV_{MERS\text{-}S\text{-}IRES\text{-}GFP}$(VSV-G)] vector-containing
181 supernatant to express MERS-S and the green marker protein GFP ($JAWSII_{green}$-MERS-S, EL-
182 4_{green}-MERS-S, $DC2.4_{green}$-MERS-S, and $DC3.2_{green}$-MERS-S), thereby presenting respective
183 peptides via MHC-I. EL-4 cells were alternatively transduced with [$HIV_{TurboFP635}$(VSV-G)]
184 vectors (59) to express red-fluorescent Katushka protein as negative control ($EL\text{-}4_{red}$). For this
185 purpose, 1×10^5 target cells were seeded in 24-well plates and transduced with 0.1, 1, or 10 µl of
186 concentrated vector suspension. For analysis of transduction efficiencies, cells were fixed in 1%
187 paraformaldehyde (Merck Millipore, Darmstadt, Germany), and the percentage of GFP- or
188 Katushka-positive cells was quantified by flow cytometry using an LSRII flow cytometer (BD,
189 Heidelberg, Germany). Cell populations revealing a 1-10% fraction of GFP-positive cells were
190 used for single cell cloning by limiting dilution. For that purpose, cell dilutions with 50 µl
191 conditioned medium statistically containing 0.3 cells were seeded per well in 96-well plates.
192 Single cells clones were cultured and analyzed by flow cytometry. GFP-positive clones were
193 selected for further analysis.

194

195 **Viruses**

196 The viruses were rescued as described (54). In brief, 5 µg of MV genome plasmids with MERS-
197 CoV-antigen ORFs were co-transfected with plasmids pCA-MV-N (0.4 µg), pCA-MV-P (0.1
198 µg), and pCA-MV-L (0.4 µg) encoding MV proteins necessary for genome replication and
199 expression in 293T cells cultured in 6-well plates using Lipofectamine 2000 (Invitrogen Life
200 Technology). The transfected 293T cells were overlaid two days after transfection onto 50%
201 confluent Vero cells seeded in 10 cm-dishes. Overlay cultures were closely monitored for

isolated syncytia indicating monoclonal replicative centers. Single syncytia were picked and overlaid onto 50% confluent Vero cells cultured in 6-well plates and harvested as "passage 0" (P0) by scraping and freeze-thaw cycle of cells at the time of maximal infection. Subsequent passages were generated after $TCID_{50}$ titration of infectious virus according to the method of Kaerber and Spaerman (60) and infection of Vero cells at an MOI = 0.03. The viruses were passaged up to P10. MERS-vaccine viruses and control viruses MV_{vac2}-GFP(H) and MV_{vac2}-GFP(P) in P3 were used for characterization, viruses in P4 for vaccination. MERS-CoV (isolate EMC/2012) (1) used for neutralization assay and challenge was propagated in Vero cells and titrated as described above for recombinant MV. All virus stocks were stored in aliquots at -80°C.

Measles virus genome sequence analysis

The RNA genomes of recombinant MV in P3 or P10 were isolated using the QIAamp RNeasy Kit (QIAgen, Hilden, Germany) according to manufacturers´ instructions and resuspended in 50 µl RNase-free water. Viral cDNA was reversely transcribed using Superscript II RT kit (Invitrogen) with 2 µl vRNA as template and random hexamer primers, according to manufacturer´s instructions. For specific amplification of antigen ORFs, the respective genomic regions of recombinant MV were amplified by PCR using primers binding to sequences flanking the regions of interest and cDNA as template. Detailed description of primers and procedures are available upon request. The PCR products were directly sequenced (Eurofins Genomics, Ebersberg, Germany).

Western Blot Analysis

For Western Blot analysis, cells were lysed and immunoblotted as previously described (61). A rabbit anti-MERS-CoV serum (1:1,000) was used as primary antibody for MERS-CoV-S and a

Journal of Virology

rabbit anti-MV-N polyclonal antibody (1:25,000) (Abcam) for MV-N detection. A donkey HRP-coupled anti-rabbit IgG (H&L) polyclonal antibody (1:10,000) (Rockland, Gilbertsville, PA) served as secondary antibody for both. Peroxidase activity was visualized with an enhanced chemiluminescence detection kit (Thermo Scientific, Bremen, Germany) on Amersham Hyperfilm ECL (GE Healthcare, Freiburg, Germany).

Production of recombinant soluble MERS-CoV spike protein

The S protein lacking the transmembrane domain was genetically tagged with 6 His residues at its carboxyterminus. The resulting construct was inserted into a Semliki Forest Virus derived self-replicating RNA vector (SFV replicon) downstream of the subgenomic promoter. These replicons were transcribed *in vitro* and purified as previously described (62, 63). Integrity of purified replicon was assessed by on-chip electrophoresis (2100 BioAnalyzer; Agilent, Santa Clara, CA). To produce SFV vector particles, replicon RNA and helper RNA were co-electroporated into BHK21 cells using a square-wave electroporator (one pulse, 750 V/cm of 16 ms; BTX ECM 830; Harvard Apparatus, Holliston, MA). Particles were harvested after 24 h, frozen in N_2(l), and stored at -80°C. For protein production, 2×10^7 BHK21 were transduced with SFV particles (MOI = 40) and harvested after 24 h. Cell pellets were lysed (PBS, 0.2% Triton X-100, Protease Inhibitor Cocktail (Roche)) for 30 min at 4°C. Afterwards, cells were sonificated and lysates were cleared by centrifugation (30 min, 21,000 × g, 4°C). The supernatant was filtered (0.2 µm), loaded on a HisTrap HP column (17-5247-01; GE Healthcare) and washed with 10 vol binding buffer (20 mM Na_2HPO_4, 0.5 M NaCl, 10 mM imidazol). S protein was eluted with binding buffer containing 0.5 M imidazol by gradient, followed by buffer exchange to PBS. Protein integrity was checked by Western blot analysis, using a mouse anti-His mAb (1:50; Dianova, Germany).

Animal experiments

All animal experiments were carried out in compliance with the regulations of the German animal protection law and have been authorized by the RP Darmstadt. Six- to 12-week-old IFNAR$^{-/-}$-CD46Ge mice expressing human CD46 (46) were inoculated intraperitoneally (i.p.) with 1×10^5 $TCID_{50}$ of recombinant MV or 200 µl OptiMEM on days 0 and 28, and bled via the retrobulbar route on days 7, 28, and 32 or 49 p.i. under anesthesia. Serum samples were stored at -20°C. Mice were euthanized on days 32 or 49 p.i., and spleens were isolated. For challenge experiments, immunized mice were transduced i.n. on day 63 with 20 µl of an adenoviral vector encoding human DPP4 and mCherry with a final titer of 2.5×10^8 PFU per inoculum (AdV-hDPP4, ViraQuest Inc.) and challenged i.n. with 20 µl of MERS-CoV with a final titer of 7×10^4 $TCID_{50}$ on day 68. The mice were euthanized 4 d after challenge and representative lung samples of the left lobe were prepared for RNA isolation.

Antibody ELISA

MV bulk antigens (10 µg/ml; Virion Serion, Würzburg) or recombinant MERS-S protein (20 µg/ml) were coated in 50 µl carbonate buffer (Na_2CO_3 30 mM; $NaHCO_3$ 70 mM; pH 9.6) per well on Nunc Maxisorp® 96 well ELISA plates (ebioscience) and incubated overnight at 4°C. The plates were washed three times with 150 µl ELISA washing buffer (PBS, 0.1% Tween 20 (w/v)) and blocked with 50 µl Blocking buffer (PBS; 5% BSA; 0.1% Tween 20) for 2 h at room temperature. Mice sera sampled on days -7 or 49 were serially diluted in ELISA dilution buffer (PBS, 1% BSA, 0.1% Tween 20), and 50 µl/well were used for the assay. The plates were incubated at 37°C for 2 h and washed again with ELISA washing buffer. Plates were incubated

with 50 µl/well of HRP conjugated rabbit anti-mouse IgG (Dako, 1:1000 in ELISA dilution buffer) at room temperature for 1 h. Subsequently, the plates were washed and 100 µl TMB substrate (ebioscience) were added per well. The reaction was stopped by addition of 50 µl/well H_2SO_4 (1 N) and the absorbance at 405 nm was measured.

Neutralization Assays

For quantification of virus neutralizing titers (VNT), mouse sera were serially diluted in two-fold dilutions in DMEM. 50 pfu of MV_{vac2}-GFP(P) or 200 $TCID_{50}$ of MERS-CoV were mixed with serum dilutions and incubated at 37°C for 1 h. Virus suspensions were added to 1×10^4 Vero cells seeded 4 h prior to assay in 96-well plates and incubated for 4 d at 37°C. Virus neutralizing titers (VNT) were calculated as reciprocal of the highest dilution abolishing infection.

ELISpot Assays

Murine IFN-γ ELISpot assays were purchased (ebioscience, Frankfurt, Germany) and performed according to manufacturer´s instructions using Multiscreen-IP ELISPOT PVDF 96-well plates (Millipore, Darmstadt, Germany). 5×10^5 splenocytes isolated 4 d after boost immunization were co-cultured with 5×10^4 $JAWSII_{green}$-MERS-S, $DC2.4_{green}$-MERS-S, or $DC3.2_{green}$-MERS-S, or the untransduced DCs for 36 h in 200 µl RPMI (10% FBS; 2 nM L-Gln; 1% Penicillin/Streptomycin). Medium alone served as negative control. 10 µg/ml concanavalin A (ConA) (Sigma Aldrich) was used for demonstration of splenocyte reactivity. 10 µg/ml recombinant MV bulk antigens (Virion Serion, Würzburg, Germany) were used to analyze MV-specific immune responses in vaccinated animals. Cells were removed from the plates and the plates incubated with biotin-conjugated anti-IFN-γ antibodies and avidin-HRP according to

manufacturer´s instructions. AEC substrate solution for development of spots was prepared according to manufacturer´s instructions using 3-amino-9-ethyl-carbazole (Sigma-Aldrich) dissolved in N,N-dimethylformamide (Merck Millipore). Spots were counted using an Eli.Scan ELISpot Scanner (A.EL.VIS, Hamburg, Germany) and ELISpot Analysis Software (A.EL.VIS).

T cell proliferation assay

Splenocytes isolated three weeks after booster immunization were labeled with 0.5 µM carboxyfluorescein-succinimidyl-ester (CFSE) (ebioscience) as previously described (64). In brief, 5×10^5 labelled cells were seeded in RPMI 1640 supplemented with 10% mouse serum, 2 nM L-Glutamin, 1 mM HEPES, 1% penicillin/streptomycin, and 2-mercaptoethanol [100 µM] in 96-wells. 200 µl Medium containing ConA [10 µg/ml], MV bulk antigens [10 µg/ml] or 5×10^3 $JAWSII_{green}$-MERS-S cells were added to each well, and cells were cultured for 6 d. Medium and untransduced JAWSII cells served as controls. Stimulated cells were subsequently stained with CD3-PacBlue (clone 500A2; Invitrogen Life Technologies; 1:50) and CD8-APC (clone 53-6.7; ebioscience; 1:100) antibodies and fixed with 1% PFA (in PBS). Stained cells were analyzed by flow cytometry using an LSR II flow cytometer (BD) and FACS Diva software (BD).

CTL killing assay

For re-stimulation of T cells isolated 4 d after booster immunization, 5×10^6 splenocytes were co-cultured with 5×10^4 $JAWSII_{green}$-MERS-S cells for 6 d in 12-wells in RPMI 1640 supplemented with 10% FBS, 2 nM L-Glutamin, 1 mM HEPES, 1% penicillin/streptomycin, 2-mercaptoethanol [100 µM], and 100 U/ml rIL-2 (murine, Peprotech). 2×10^3 $EL\text{-}4_{red}$ cells were labeled with 0.5 µM CFSE and mixed with 8×10^3 $EL\text{-}4_{green}$-MERS-S cells per well. Splenocytes were counted and co-

cultured with EL-4 target cells at the indicated ratios for 4 h. Afterwards, EL-4 cells were labeled with Fixable Viability Dye eFluor® 780 (ebioscience), fixed with 1% PFA, and analyzed by flow cytometry using an LSR II flow cytometer (BD) and FACS Diva software (BD). For indication of Antigen:NC EL-4 ratio the cell count of living MERS-S expressing cells was divided by the population of living negative controls.

Determination of viral RNA copy numbers and infectious virus in mouse tissue

Samples of immunized and challenged mice, i.e. 6x6 mm tissue slices of approx. 0.035±0.011 g weight excised from the center of the left lung lobe, were homogenized in 1 ml DMEM with ceramic beats with a diameter of 1.4 mm in a FastPrep^{TM} SP120 instrument for 3 × 40 s at 6.5 m/s. The homogenate was centrifuged for 3 min at 2,400 rpm in a Mikro 200R centrifuge (Hettich Lab Technology) to remove tissue debris. Live viruses titers in supernatant ($TCID_{50}$/ml) were determined on Vero cells as described above. 100 µl of the supernatants were used for RNA isolation with the RNeasy Mini Kit (QIAgen) according to the manufacturer's instruction. RNA amount was measured with the NanoDrop ND-100 Spectrophotometer. Total RNA was reversely transcribed and quantified by real time PCR using SuperScript III OneStep RT-PCR System (Invitrogen Life Technologies) as described previously (65) with the primer upE-Fwd and upE-Rev and the probe upE-Prb on the ABI7900 HT Fast Real Time PCR System (Life Technologies Instruments).

Additionally, for every sample of the transduced and infected mice, evidence for successful hDPP4 transduction was determined by real time RT-PCR for mCherry with the OneStep RT-PCR Kit on the Rotor Gene Q (both Qiagen). Primers and probe (Tib-Molbiol, Berlin, Germany) were as follows: mCherry forward: CATGGTAACGATGAGTTAG, mCherry reverse: GTTGCCTTCCTAATAAGG, and mCherry probe: FAM (6-carboxyfluorescein)–

343 TACCACCTTACTTCCACCAATCGG–BBQ (BlackBerry®Quencher). Primers and probe were
344 used in final concentrations of 0.4 µM and 0.2 µM, respectively. qRT-PCR program was as
345 follows: 50°C for 30 min, 95°C for 15 min, 40 cycles of 95°C for 15 s, 48°C for 30 s, and 72°C
346 for 20 s. All samples for mCherry were evaluated in one run to exclude an impact of different
347 conditions on the results in different runs. Quantification was carried out with a standard curve
348 based on 10-fold serial dilutions of appropriate cloned RNA ranging from 10^2 to 10^5 copies.
349 Briefly, PCR fragments were generated using the primers described above. For cloning, the
350 TOPO TA Cloning Kit with pCR2.1-TOPO plasmid (Invitrogen) and *E. coli* were used. Inserts
351 were examined for correct orientation and length and were amplified with plasmid-specific
352 primers, purified, and transcribed into RNA with SP6/T7 Transcription Kit (Roche).
353
354 **Histopathological and immunohistochemical examination of lung tissue**
355 Lungs of vaccinated and mock vaccinated mice transduced with AdV-hDPP4 were collected on
356 day 4 post challenge with MERS-CoV. Tissue was fixed in 4% paraformaldehyde and embedded
357 in paraffin. Sections were cut with a Leica RM2255 microtome (Leica Biosystems) and stained
358 with hematoxylin and eosin (H&E). For detection of MERS-CoV, a rabbit polyclonal antibody
359 against MERS-CoV spike protein S1 (100208-RP; Sino Biological Inc, Beijing, CN) diluted 1:50
360 was used. To monitor adenovirus transduction, a mouse monoclonal antibody against mCherry
361 (ab125096; Abcam, Cambridge, UK) diluted 1:250 was used after antigen retrieval with Target
362 Retrieval Solution (Dako) for 23 min at 97°C. To block unspecific binding, slides were incubated
363 for 10 min with 20% nonimmune pig serum (MERS-CoV) or for 30 min with 20% nonimmune
364 horse serum (mCherry). Primary antibodies were incubated overnight at 4°C. A pig anti-rabbit
365 IgG and a biotinylated horse anti-mouse IgG served as secondary antibodies for MERS-CoV and
366 mCherry, respectively. For detection of antigen-antibody complexes, the ABC-method for

mCherry and the rabbit PAP-method for MERS-CoV were used in combination with DAB for staining. Papanicolaou stain was used for counterstaining.

Statistical analysis

To compare the means of different groups in growth curves, neutralization assay and ELISpot, a non-parametric One-way ANOVA was performed. For proliferation assay the mean differences between control and vaccinated groups were calculated and analysed by unpaired t test. To all three groups in CTL killing assays a linear curve was fitted for antigen vs. logarithmised effector-target ratio E:T. The p values testing for differences in slopes were calculated and MERS-S(H) or MERS-solS(H) compared with control ATU. The P values were not adjusted for multiplicity due to the explorative character of the study. For analysis of challenge data, mean ratios and 95% Confidence Intervals were calculated based on logarithmised and back-transformed data. The ratio instead of the difference was chosen due to the rather log-normal distribution of the data. Width of the confidence intervals caused by high variability of the data and limited sample size (N = 10 observations each). For comparisons between groups the Wilcoxon's 2-Sample Test was used. P values were not adjusted for multiple comparisons due to the explorative character of the study.

Results

Generation and expression of MERS-CoV-S by recombinant MV_{vac2}

Since the spike protein (S) of SARS-CoV has been shown to potently induce humoral and cellular immune responses, MERS-S was chosen as appropriate antigen to be expressed by the recombinant MV vaccine platform. In addition to full-length MERS-S, a truncated form lacking the transmembrane and cytoplasmic domains (solS) was cloned into two different additional

transcription units (ATUs) either behind P (post P) or H (post H) cassettes of vaccine strain MV_{vac2} genome (Fig. 1A). Virus clones of all recombinant genomes were successfully rescued and amplified up to passage 10 (P10) in Vero cells with titers of up to 6×10^7 $TCID_{50}$/ml. The stability of the viral genomes was demonstrated via sequencing of viral genomes after RT-PCR (data not shown). Besides the exclusion of mutations or deletions of the antigen-encoding genes, the verification of antigen expression is essential for vaccine function and, thus, virus characterization. Western blot analysis of Vero cells infected with the different MV_{vac2}-MERS vaccines revealed expression of the antigen (Fig. 1B). Interestingly, the expression of both S and solS was higher when cells were infected with viruses encoding antigens in post-H ATU compared to the post-P constructs. Therefore, growth kinetics were analyzed to check if the insertion or expression of the S antigen variants into or by recombinant MV, respectively, may impair the vaccines´ replication (Fig. 1C, D). For that purpose, the vaccine viruses containing the MERS-S or MERS-solS gene in post H (Fig. 1C) or post P (Fig. 1D) positions were analyzed in parallel to respective MV_{vac2}-GFP control viruses. MV_{vac2} encoding full-length, membrane-bound MERS-S grew comparably to the control viruses; only MV_{vac2}-MERS-solS(P) (Fig. 1D) and MV_{vac2}-MERS-solS(H) (Fig. 1C) revealed an approx. 3-fold reduced maximal virus titer, albeit no statistical significance could be observed (1.5×10^5 $TCID_{50}$/ml for MV_{vac2}-MERS-solS(P) and 4.7×10^5 $TCID_{50}$/ml for MV_{vac2}-MERS-solS(H) *vs.* 4.7×10^5 for MV_{vac2}-GFP(P) and 1.2×10^6 $TCID_{50}$/ml for MV_{vac2}-GFP(H)) (Fig. 1C). Thus, cloning and rescue of MVs expressing MERS-CoV antigens, even at the cost of 4049 bp additional genome length, was achieved easily and relative quickly. All constructs expressed the inserted antigens without significant impact on viral replication.

Journal of Virology

Antibodies with neutralizing capacity directed against MV or MERS-CoV are induced by MV_{vac2}-MERS-S and MV_{vac2}-MERS-solS

To test the efficacy of the MV_{vac2}-MERS vaccines *in vivo,* genetically modified $IFNAR^{-/-}$-CD46Ge mice were chosen, since they are the prime small animal model for analysis of MV-derived vaccines (46). Based on the higher antigen expression of MERS-S and MERS-solS if cloned into the post-H position of the MV genome, the respective viruses were used for vaccination. Thus, 6 mice per group were inoculated via the intraperitoneal (i.p.) route on days 0 and 28 with each time 1×10^5 $TCID_{50}$ of MV_{vac2}-MERS-S(H), MV_{vac2}-MERS-solS(H), or MV_{vac2}-ATU(P), the latter a recombinant control virus without insertion of a foreign antigen-encoding gene cassette into an otherwise empty additional transcription unit. Medium-inoculated mice served as negative controls. 21 days after boost immunization, sera of immunized mice were analyzed in comparison to pre-bleed sera by ELISA on antigen-coated plates for antibodies binding to MV bulk antigens or MERS-S (Fig. 2A,B). Indeed, sera of mice vaccinated with MV_{vac2}-MERS-S(H) or MV_{vac2}-MERS-solS(H) clearly encompassed IgG binding to MERS-S (Fig. 2B), whereas no antibodies were found in mice before vaccination (Fig. 2A), or in control mice. Moreover, sera of mice vaccinated with any recombinant MV had IgG in the serum binding to MV bulk antigens, as expected, indicating successful vaccination with MVs and general mouse reactivity. To determine the neutralizing capacity of the induced antibodies, sera dilutions´ potential to neutralize 200 $TCID_{50}$ of MERS-CoV or 50 plaque-forming units (PFU) of MV_{vac2}-GFP(H) (Fig. 3A-C) was assayed. All mice immunized with recombinant MV (including the control virus) indeed developed MV virus neutralizing titers (VNT) already after the first immunization (Fig. 3B). These titers were boosted approx. 6-fold upon the second immunization (512 to 3072 VNT, Fig. 3C). Evidence for induction of neutralizing antibodies against MERS-CoV was only found in mice vaccinated with MV_{vac2}-MERS-S(H) or MV_{vac2}-MERS-solS(H), as

expected. VNT against MERS-CoV reached a titer of 96 to 167 after the first immunization (Fig. 3B) and was boosted about 5-7-fold by the second immunization (Fig. 3C). Mice immunized with MV_{vac2}-MERS-S(H) induced slightly higher MERS-CoV VNTs compared to MV_{vac2} expressing the truncated form of the spike protein (167 *vs.* 96 after the first and 874 *vs.* 640 after the second immunization) (Fig. 3B, C). However, this difference was not statistically significant. No VNTs against MV or MERS-CoV were detected in control mice inoculated with medium alone. In summary, both recombinant MVs expressing MERS-S or MERS-solS specifically induced significant amounts of antibodies in immunized mice capable to neutralize MV as well as MERS-CoV.

Splenocytes of animals vaccinated with MV_{vac2}-MERS-S or MV_{vac2}-MERS-solS secrete IFN-γ upon MERS-S specific stimulation

To analyze the ability of MV-based vaccine viruses to induce MERS-CoV-specific cellular immune responses, splenocytes of animals vaccinated with MV_{vac2}-MERS-S(H), MV_{vac2}-MERS-solS(H), or control animals inoculated with medium or MV_{vac2}-ATU(P) were analyzed for antigen-specific IFN-γ secretion by ELISpot assay. For this purpose, mice were immunized following the described prime-boost scheme, and splenocytes were isolated four days after the second immunization. To re-stimulate the antigen-specific T cells *in vitro*, syngeneic murine DC cell lines (JAWSII, DC2.4, and DC3.2) had been genetically modified by lentiviral vector transduction to stably express MERS-S protein and thereby to present the respective T cell epitopes on MHC. Single cell clones were derived by flow cytometric sorting of single GFP-positive cells. Antigen expression by transduced DCs was verified by Western Blot analysis (data not shown).

ELISpot assays using splenocytes of vaccinated animals in co-culture with JAWSII-MERS-S revealed about 2,400 IFN-γ secreting cells per 1×10^6 splenocytes after immunization with MV_{vac2}-MERS-S or MV_{vac2}-MERS-solS (Fig. 4A). In contrast, control mice revealed a background response of about 200 IFN-γ producing cells per 1×10^6 splenocytes. As expected, re-stimulation of T cells by JAWSII presenting no exogenous antigen revealed only reactivity in the range of background (Fig. 4A). To rule out clonal or cell line-associated artifacts, antigen-specific IFN-γ secretion by splenocytes of MV_{vac2}-MERS-S or MV_{vac2}-MERS-solS vaccinated mice was confirmed by stimulation with transgenic DC2.4 (Fig. 4B) or DC3.2 (Fig. 4C) cell clones expressing MERS-S. These cell lines stimulated 1,200 to 2,300 IFN-γ secreting cells per 1×10^6 splenocytes in animals receiving the recombinant MERS vaccines, whereas no background stimulation of respective controls was observed. The differences between MV control and MV_{vac2}-MERS-S or MV_{vac2}-MERS-solS vaccinated mice were significant for all cell lines. Additionally, cellular immune responses targeting MV antigens were detected upon stimulation with MV bulk antigens in vaccinated mice that had received any recombinant virus, as expected. However, MV bulk antigens stimulated only about 930 to 1,500 IFN-γ secreting cells per 1×10^6 splenocytes of MV vaccinated animals. Finally, splenocytes of all mice revealed a similar basic reactivity to unspecific T cell stimulation, as confirmed by similar numbers of IFN-γ secreting cells upon ConA treatment (Fig. 4D). Remarkably, both stimulation by ConA or MV bulk antigens resulted in lower numbers of IFN-γ^+ cells than stimulation by DCs expressing MERS-S, indicating an extremely robust induction of cellular immunity against this antigen. Thus, the generated MV-based vaccine platform expressing MERS-S or MERS-solS not only induces humoral, but also strong MERS S-specific cellular immune responses.

Journal of Virology

MV_{vac2}-MERS-S(H) or MV_{vac2}-MERS-solS(H) induce antigen specific $CD8^+$ CTLs

While ELISpot analyses revealed antigen-specific IFN-γ secretion by vaccinated mice´ T cells, we next aimed at detecting antigen-specific $CD8^+$ CTLs which would be important for clearance of virus infected cell. For that purpose, proliferation of $CD8^+$ T cells upon stimulation with MERS-S was analyzed 3 weeks after the boost via a flow cytometric assay. Mice were immunized as described and splenocytes were isolated 21 days after the boost. JAWSII cells expressing MERS-S were used for re-stimulation of MERS-S-specific T cells. The splenocytes were labelled with CFSE and subsequently co-cultured with JAWSII-MERS-S cells or, as a control, with parental JAWSII cells for 6 d and finally stained for CD3 and CD8 before being analyzed by FACS for proliferation, detectable by the dilution of the CFSE stain due to cell division.

T cells of mice vaccinated with MV_{vac2}-MERS-S or MV_{vac2}-MERS-solS revealed an increase in the population of $CD3^+CD8^+CFSE^{low}$ cells after re-stimulation with JAWSII-MERS-S cells compared to re-stimulation with parental JAWSII without MERS antigens (Fig. 5A). In contrast, T cells of control mice did not reveal this pattern, but the $CFSE^{low}$ population remained rather constant, as expected. This specific increase in $CD3^+CD8^+CFSE^{low}$ cells, which was significant for MV_{vac2}-MERS-S and nearly significant ($P = 0.0505$) for MV_{vac2}-MERS-solS vaccinated mice, indicates that $CD3^+CD8^+$ cytotoxic T lymphocytes (CTLs) specific for MERS-S have proliferated upon respective stimulation. Thus, MERS-specific cytotoxic memory T cells are induced in mice after vaccination with MV_{vac2}-MERS-S(H) or MV_{vac2}-MERS-solS(H).

Induced T cells reveal antigen-specific cytotoxicity.

To demonstrate the effector ability of induced CTLs, a killing assay was performed to directly analyze antigen-specific cytotoxicity (Fig. 5B). Splenocytes of immunized mice isolated 4 days

post booster vaccination were co-cultured with JAWSII-MERS-S or the non-transduced control JAWSII cells for 6 d to re-stimulate antigen-specific T cells. When these re-stimulated T cells were co-incubated with a defined mixture of EL-4_{green}-MERS-S target and EL-4_{red} control cells (ratio 4:1), only T cells from MV_{vac2}-MERS-S(H) or MV_{vac2}-MERS-solS(H)-vaccinated mice significantly shifted the ratio of live MERS-S-expressing target cells to control cells in a dose dependent manner (Fig. 5B). This antigen-dependent killing was also dependent on re-stimulation with JAWSII-CoV-S cells, since naïve T cells did not shift significantly the ratios of target to non-target cells.

These results indicate that CTLs isolated from MV_{vac2}-MERS-S(H) or MV_{vac2}-MERS-solS(H) vaccinated mice are capable of lysing cells expressing MERS-S. Neither splenocytes of control mice re-stimulated with JAWSII-MERS-S nor splenocytes of MERS-S vaccinated mice re-stimulated with control JAWSII cells showed such an antigen-specific killing activity. These results demonstrate that the MV-based vaccine platform induces fully functional antigen-specific $CD8^+$ CTLs in vaccinated mice when being applied as MERS-CoV vaccine.

Vaccination of mice with MV_{vac2}-MERS-S(H) or MV_{vac2}-MERS-solS(H) rescues animals from challenge with MERS-CoV

The induction of strong humoral and cellular immune responses directed against MERS-CoV in mice vaccinated with MV_{vac2}-MERS-S(H) or MV_{vac2}-MERS-solS(H) indicated that those animals are possibly protected against a challenge with MERS-CoV. To investigate efficacy of the candidate vaccines, two independent experiments were performed where groups of five mice were either vaccinated with MV_{vac2}-MERS-S(H), MV_{vac2}-MERS-solS(H), control MV (MV_{vac2}-ATU(P)), or left untreated. All mice immunized with MV_{vac2}-MERS-S(H) or MV_{vac2}-MERS-solS(H) showed VNTs directed against MERS-CoV with titers up to 1,280 for MERS-S and up to

960 for MERS-solS. No MERS-CoV neutralizing antibodies were detected in control mice (data not shown). Since the murine DPP4 does not serve as a functional MERS-CoV entry receptor (66) and mice are therefore not susceptible to MERS-CoV infection**,** the vaccinated mice were intranasally (i.n.) transduced with a recombinant adenoviral vector to express human DPP4 (AdV-hDPP4) in murine airways. At five d after airway transduction with AdV-hDPP4, mice were infected i.n. with 7×10^4 $TCID_{50}$ MERS-CoV. Four days later, animals were euthanized, lungs isolated, the tissue homogenized and homogenates used for purification of total RNA and virus titration. In the lungs of mock control mice, MERS-CoV RNA was detected by qRT-PCR (9,649 ± 3,045 MERS-CoV genome copies/ng RNA; Fig. 6A). Mice vaccinated with control MV_{vac2}-ATU(P) showed slightly lower copy numbers of viral RNA (5,923 ± 3,045 MERS-CoV genome copies/ng RNA; Fig. 6A). Vaccination with MV_{vac2}-MERS-S(H) or MV_{vac2}-MERS-solS(H) resulted in near-complete reduction of viral loads to 74 ± 60 genome copies/ng RNA or 51 ± 32 genome copies/ng RNA, respectively (Fig. 6A). Next, titers of infectious virus were determined in the lung tissue. While the titers were generally low, they corresponded to the qRT-PCR data. In mock control mice, titers of up to 5,000 $TCID_{50}$/ml were determined (Mean: 868 ± 692 $TCID_{50}$/ml) and in lungs of mice vaccinated with the vaccine backbone without MERS antigen (MV_{vac2}-ATU(P)), 1,673 ± 866 $TCID_{50}$/ml were detected. A considerable albeit statistically not significant reduction of infectious virus titers was found in mice vaccinated with MV_{vac2}-MERS-S(H) or MVvac2-MERS-solS(H) compared to mock control mice (Fig. 6B). These results revealed that, indeed, vaccination with the recombinant measles viruses was able to protect mice against a challenge with MERS-CoV.

MERS-CoV infection of transduced mice was not always successful, which was indicated by a completely negative PCR result for viral genomes in about 40% of all animals. In approximately 30% of MERS-CoV negative animals, PCR for the mCherry gene was negative indicating that

transduction was not successful and explaining why these mice were not susceptible. Why the remaining transduced mice were not infected is currently unclear. However, even when the drop-out animals were included in statistical analysis, the difference between mean viral loads of the medium control group and MV_{vac2}-MERS-solS(H) (ratio: 278.2, 95% CI 1.52 – 50,904) treated animals stayed significant (P = 0.0329). Protection of the MV_{vac2}-MERS-S(H) vaccinated group was close to significance (P = 0.057) compared to mock animals (ratio 149.2, 95% CI 0.82 – 27,301).

Histological analyses were performed to analyse if the reduced viral load in mice vaccinated with MV_{vac2}-MERS-solS(H) or MV_{vac2}-MERS-S(H) was matched by less pathological changes in mouse lungs (Fig. 7). For this purpose, lungs were examined with H&E staining to visualize inflammation. Additionally, MERS-S and mCherry expression was determined by immunohistochemistry using antigen-specific antibodies. Consistent with qRT-PCR, all mice that were positive in qRT-PCR for the mCherry gene expressed mCherry in epithelia of the lungs demonstrating successful transduction (Fig. 7, right column). The histopathological examination of H&E-stained lung tissues clearly showed differences between the vaccinated mice and controls (Fig. 7, left column). In the mock (OptiMEM) as well as vector control (MV_{vac2}-ATU(P)) groups, large areas of inflamed tissue were observed densely packed with lymphocytes, macrophages, and, to a lesser extent, neutrophils and eosinophils. Moreover, hyperplasia of the bronchus-associated lymphoid tissue was present at various degrees. These inflamed areas co-localized with expression of MERS-CoV spike protein (Fig. 7, middle column). Mice that were vaccinated with recombinant MV expressing MERS S showed less signs of inflammation and consistently less MERS-S expression after challenge with MERS. These differences were most obvious in lungs of MV_{vac2}-MERS-solS(H) vaccinated animals, where only small foci of

Journal of Virology

580 inflammation could be observed. These results revealed that vaccination with recombinant MV
581 expressing MERS S reduced pathological changes in the lungs of MERS-CoV infected mice.
582
583 **Discussion**
584 In this study, we have demonstrated the capacity of recombinant MV encoding different forms of
585 the MERS-CoV S glycoprotein to induce both strong humoral and cellular immune responses that
586 revealed protective capacity in a challenge model of mice vaccinated with these stable life-
587 attenuated vaccines. So far, different strategies to develop vaccines against MERS-CoV have
588 been proposed including recombinant full-length S protein (67) or the receptor-binding domain
589 (RBD) of MERS-S (27, 28, 30, 31, 68), as well as platform-based approaches using modified
590 vaccinia virus Ankara (MVA, (22)) or adenoviral vectors (AdV, (23)) encoding MERS-S. Similar
591 to our MV-based vaccine, these experimental vaccines induced humoral immune responses with
592 virus-neutralizing capacity. Among vectored vaccines, immunization with MVA or AdV
593 expressing MERS-S resulted in VNTs in the range of 1,800 or 1,024, respectively, when used to
594 immunize Balb/c mice. Vaccination with MV_{vac2}-MERS-S or MV_{vac2}-MERS-solS induced
595 somewhat lower VNTs of about 840, which is an extremely robust titer taking into account that
596 mice were immunized with 10^3-fold fewer virus particles compared to MVA, and 10^6-fold lower
597 particles than replication-deficient AdV. Moreover, transgenic $IFNAR^{-/-}$-CD46Ge mice have
598 been used in our study with defects in type I IFN receptor signaling. Knock-out of the type I IFN
599 receptor results in reduced adaptive immune responses (68–70) since type I IFNs are an
600 important link between the innate and adaptive immunity via, among others factors, activation of
601 DC (71), giving those mice´ adaptive immune system some disadvantage. Nevertheless, these
602 mice have to be used routinely to analyze efficacy of MV-based vaccines in a small animal model
603 (46), since wt mice are not susceptible to MV infection for mainly two reasons: Firstly, murine

604 homologues of MV receptors cannot be used for cell entry (69) with the exception of nectin-4
605 (70). Secondly, MV replication is strongly impaired by type I IFN responses (71, 72), and mice
606 with intact IFNAR feedback loop failed to be susceptible to MV infection (46). Therefore, the
607 IFNAR$^{-/-}$-CD46Ge mouse strain transgenic for human MV vaccine receptor CD46 and with a
608 knock-out of the IFNAR is used to analyze MV-based vaccines. Additionally, the mouse strain
609 backgrounds (Balb/c *vs.* C57BL/6) differ in T helper cell responses (BALB/c, predominantly
610 Th2; C57BL/6, Th1 responses (73)), which reflects in different balance of cellular *vs.* humoral
611 immunity (74, 75). Thus, the mouse model which had to be used in this study certainly is
612 disadvantageous with respect to VNTs. To directly compare efficacy of the different vector
613 systems, all vectors should ideally be used side-by-side in the same animal model. This may be a
614 focus of future studies. The VNT of about 1,000 induced by three immunizations with
615 recombinant RBD are hardly comparable to our results since other protocols for determination of
616 VNT were used in these studies (27, 31). Interestingly, the expression of the soluble version of S
617 by MV did not enhance VNTs. This is consistent with humoral immunity induced by DNA
618 vaccines targeting SARS-CoV. Plasmids encoding soluble SARS-S lacking the transmembrane
619 domain provoked lower VNTs than membrane-bound variants (32). An altered, less physiological
620 conformation of the S protein has been proposed to result from deletion of the transmembrane
621 domain, which should be responsible for worse immune recognition and lower antibody titers
622 binding to the native, correctly folded S proteins in virus particles. In contrast, the soluble S1
623 domain of MERS-S expressed by AdV actually induced slightly higher VNTs compared to full-
624 length S (23). However, soluble constructs consisting of the MERS-S1 and S2 domain have not
625 been compared to soluble S1 domain, yet. Interestingly, recombinant MV expressing soluble
626 MERS-S revealed slightly impaired replication in comparison to control MV, in contrast to MV
627 expressing full-length MERS-S. This impaired viral replication might base on cytotoxicity of

MERS-solS, probably as a result of an altered folding or the solubility of the S protein. Cytotoxic effects of the S protein have already been observed for the S2 domain of SARS-S (76–80), but not for other coronaviruses like MHV (81). Though, both MV-based vaccines encoding either the soluble or the full-length variant of MERS-S did induce strong VNTs and cellular immune responses.

The protective capacity of humoral immune responses against CoV infection is controversially discussed. Neutralizing antibodies have been identified as correlates of protection against SARS-CoV challenge, since passive serum transfer was sufficient to rescue animals from challenge (32, 82), and T cell-depletion did not impair protection (32). In contrast, immunization with the nucleocapsid protein resulted in protection against the coronavirus infectious bronchitis virus (IBV) without induction of neutralizing antibodies (83, 84), indicating the capacity of cellular immune responses for IBV protection. Anyway, the antigenic potential of S for induction of $CD4^+$ or $CD8^+$ T cell immunity has already been demonstrated for SARS-CoV (32, 85) using recombinant protein or DNA vaccines. Also for MERS-CoV, application of RBD protein together with adjuvants has been shown to induce cellular immunity (27, 31). We demonstrated here in this study induction of cellular immunity by a vectored vaccine that works independently from adjuvants or application strategy. The MV-based vaccine induced very strong MERS-S-specific $CD8^+$ T cell responses, revealed by ELISpot, killing, and proliferation assays. The broad repertoire of reactivity, in the case of antigen-specific proliferation also 21 days after the booster immunization, indicates induction of both functional effector and memory T cell repertoire by MV_{vac2}-MERS-S and MV_{vac2}-MERS-solS. Thereby, the extraordinary high number of IFN-γ secreting T cells in vaccinated mice both stresses the potential of the vaccine platform and underlines the immunogenicity of MERS-S.

651 On top, the present study tested whether the induced immune responses protected mice against a
652 challenge infection with MERS-CoV. Indeed, vaccination with MV_{vac2}-MERS-S or MV_{vac2}-
653 MERS-solS significantly reduced viral loads in the lungs of vaccinated mice after challenge with
654 MERS-CoV. As expected, this reduction of viral load correlated with reduced pathological
655 alterations in the lung, indicating that MV-derived MERS vaccines were able to confer protection
656 against MERS-CoV infection. At least 4 mice out of each group did not reveal any MERS-CoV
657 infection nor any pathological lung alterations indicating failure of infection in these individuals.
658 In 30% of those mice, transduction with the recombinant adenovirus expressing human DPP4
659 seemed to be not successful. However, the majority of mice with no signs of MERS-CoV
660 infection, at all, showed expression of mCherry indicating that transduction was successful.
661 Currently the reason of the failure to infect these animals is unclear.
662 The direct correlates of protection in the vaccinated mice remain to be determined in future
663 studies. Most recently, mice transgenic for human DPP4 have been developed, that allow analysis
664 of MERS-CoV infection on a more robust and physiologic basis (86). These could only be used
665 for analysis of MV-based vaccines after intercrossing them with $IFNAR^{-/-}$-CD46Ge or similar
666 mouse strains to gain mice simultaneously susceptible to MV and MERS-CoV, which may also
667 be a focus of future work.
668 Efficacy of MV_{vac2}-based MERS vaccines has been demonstrated in MV naïve mice.
669 Theoretically, pre-existing anti-vector immunity against the MV backbone may be considered as
670 potential limitation both for the specific MERS-vaccines tested in this study, but also of
671 recombinant MV as vaccine platform, in general, for the use in MV-immunized patients (87).
672 However, it has been clearly demonstrated both in mice (41, 45) and non-human primates (41)
673 with humoral immune responses regarded to be protective against measles, that vaccination with
674 recombinant MVs encoding antigens of HIV-1 (41) or Chikungunya virus (45) still induced

surprisingly robust antigen-specific immune responses. Most interestingly, when analyzing efficacy of recombinant MV-CHIKV vaccine in a phase I trial in human volunteers, the vaccine was recently shown to be effective in inducing anti-CHIKV immune responses irrespective of pre-existing anti-measles immunity (47). These data question the "sterilizing" character of measles immunity, and clearly indicate the potential of recombinant MV as promising vaccine platform for vaccination against MERS-CoV or other infectious agents, in general. Indeed, efficacy of MV-based recombinant vaccines has been demonstrated pre-clinically with quite a range of different pathogens´ antigens, e.g. HBV (39), Dengue virus (44), WNV (42) and CHIKV (45). Additionally, the efficacy of MV to induce immune responses against coronaviruses has been shown for the S and nucleocapsid protein of SARS-CoV (19). All these recombinant vaccines have in common that they are based on a very well know platform: MV vaccines have been shown to exhibit an extremely beneficial safety profile in the light of millions of applied doses over the last 40 years. Only heavily immune-suppressed patients are excluded from measles vaccination campaigns, but the protection holds over decades and is thought to be most likely for life (33, 34).

Most interestingly, a quite similar recombinant vaccine based on a rhabdovirus, member of another family within the *mononegavirales* order, is currently tested in the clinic as experimental vaccine against Ebola virus (EBOV) infections. Recombinant vesicular stomatitis virus (VSV) encoding the Ebola Zaire strains´ glycoprotein replacing VSV-G (VSV-ZEBOV) was shown to be effective in animal models (88, 89) and is now tested in phase I trials for safety in human patients (90), in preparation to being moved to the field to combat current EBOV epidemics. Thereby, the potential interest in such platform-based vaccines to combat emerging or re-emerging infections is impressively highlighted.

Journal of Virology

Taken together, MV vaccine strain Moraten-derived recombinant MV_{vac2} vaccines are effective vaccines against MERS-CoV, inducing both humoral and cellular immune responses protective for vaccinated animals. Thereby, the capacity of the recombinant MV-based vaccine platform for generation of fast available and effective vaccines has been demonstrated also with a more general view to future emerging or re-emerging infections, but also with view on MERS-CoV: MV-MERS-S provides an opportunity for further development of this experimental vaccine to be prepared especially for the risk of pandemic spread of this disease.

Acknowledgements

The authors would like to thank Vivian Koch, Daniela Müller, Michael Schmidt and Gotthard Ludwig for excellent technical assistance, Sonja Witzel, Manuel Gimmel, Tina Hempel, Aileen Laubenheimer, and Tobias Blödel for excellent technical support in production of recombinant MERS-S protein, and Roland Plesker for assistance in animal experiments. We thank Lucie Sauerhering and Erik Dietzel for help with animal studies in BSL-4. The authors are indebted to Ron Fouchier for providing MERS-CoV strain EMC/2012, to Kenneth Rock for DC2.4 and DC3.2 cells, and to Christian Drosten and Doreen Muth for PCR-protocols. The authors would further like to thank Bakhos Tannous for providing pCSCW2gluc-IRES-GFP and Kenneth Lundström for the SFV vector system. This work was supported by the German Center for Infection Research (DZIF; TTU 01.802, TTU 01.904) and the Deutsche Forschungsgemeinschaft (SFB1021, SFB593).

719 **References**

720 1. **Zaki AM, van Boheemen S, Bestebroer TM, Osterhaus, Albert D M E, Fouchier, Ron**
721 **A M.** 2012. Isolation of a novel coronavirus from a man with pneumonia in Saudi Arabia.
722 The New England journal of medicine **367**:1814–1820. doi:10.1056/NEJMoa1211721.
723 2. **http://www.who.int/csr/don/17-december-2014-mers/en/**.
724 3. **Drosten C, Meyer B, Müller MA, Corman VM, Al-Masri M, Hossain R, Madani H,**
725 **Sieberg A, Bosch BJ, Lattwein E, Alhakeem RF, Assiri AM, Hajomar W, Albarrak**
726 **AM, Al-Tawfiq JA, Zumla AI, Memish ZA.** 2014. Transmission of MERS-coronavirus in
727 household contacts. The New England journal of medicine **371**:828–835.
728 doi:10.1056/NEJMoa1405858.
729 4. **Petersen E, Hui DS, Perlman S, Zumla A**. Middle East Respiratory Syndrome- advancing
730 the public health and research agenda on MERS- lessons from the South Korea outbreak.
731 International journal of infectious diseases : IJID : official publication of the International
732 Society for Infectious Diseases **36**:54–55. doi:10.1016/j.ijid.2015.06.004.
733 5. **Cowling BJ, Park M, Fang VJ, Wu P, Leung GM, Wu JT**. Preliminary epidemiological
734 assessment of MERS-CoV outbreak in South Korea, May to June 2015. Euro surveillance :
735 bulletin Européen sur les maladies transmissibles = European communicable disease bulletin
736 **20**.
737 6. **Raj VS, Farag, Elmoubasher A B A, Reusken, Chantal B E M, Lamers MM, Pas SD,**
738 **Voermans J, Smits SL, Osterhaus, Albert D M E, Al-Mawlawi N, Al-Romaihi HE,**
739 **AlHajri MM, El-Sayed AM, Mohran KA, Ghobashy H, AlHajri F, Al-Thani M, Al-**
740 **Marri SA, El-Maghraby MM, Koopmans, Marion P G, Haagmans BL.** 2014. Isolation
741 of MERS coronavirus from a dromedary camel, Qatar, 2014. Emerging infectious diseases
742 **20**:1339–1342. doi:10.3201/eid2008.140663.
743 7. **Ferguson NM, Van Kerkhove, Maria D.** 2014. Identification of MERS-CoV in dromedary
744 camels. The Lancet Infectious Diseases **14**:93–94. doi:10.1016/S1473-3099(13)70691-1.
745 8. **Müller MA, Corman VM, Jores J, Meyer B, Younan M, Liljander A, Bosch B,**
746 **Lattwein E, Hilali M, Musa BE, Bornstein S, Drosten C.** 2014. MERS Coronavirus
747 Neutralizing Antibodies in Camels, Eastern Africa, 1983-1997. Emerging infectious diseases
748 **20. doi:**10.3201/eid2012.141026.
749 9. **Meyer B, Müller MA, Corman VM, Reusken, Chantal B E M, Ritz D, Godeke G,**
750 **Lattwein E, Kallies S, Siemens A, van Beek J, Drexler JF, Muth D, Bosch B, Wernery**

U, Koopmans, Marion P G, Wernery R, Drosten C. 2014. Antibodies against MERS coronavirus in dromedary camels, United Arab Emirates, 2003 and 2013. Emerging infectious diseases **20**:552–559. doi:10.3201/eid2004.131746.

10. **Corman VM, Jores J, Meyer B, Younan M, Liljander A, Said MY, Gluecks I, Lattwein E, Bosch B, Drexler JF, Bornstein S, Drosten C, Müller MA.** 2014. Antibodies against MERS coronavirus in dromedary camels, Kenya, 1992-2013. Emerging infectious diseases **20**:1319–1322. doi:10.3201/eid2008.140596.
11. **Memish ZA, Cotten M, Meyer B, Watson SJ, Alsahafi AJ, Al Rabeeah, Abdullah A, Corman VM, Sieberg A, Makhdoom HQ, Assiri A, Al Masri M, Aldabbagh S, Bosch B, Beer M, Müller MA, Kellam P, Drosten C.** 2014. Human infection with MERS coronavirus after exposure to infected camels, Saudi Arabia, 2013. Emerging infectious diseases **20**:1012–1015. doi:10.3201/eid2006.140402.
12. **Azhar EI, El-Kafrawy SA, Farraj SA, Hassan AM, Al-Saeed MS, Hashem AM, Madani TA.** 2014. Evidence for camel-to-human transmission of MERS coronavirus. The New England journal of medicine **370**:2499–2505. doi:10.1056/NEJMoa1401505.
13. **Lau, Susanna K P, Li, Kenneth S M, Tsang, Alan K L, Lam, Carol S F, Ahmed S, Chen H, Chan K, Woo, Patrick C Y, Yuen K.** 2013. Genetic characterization of Betacoronavirus lineage C viruses in bats reveals marked sequence divergence in the spike protein of pipistrellus bat coronavirus HKU5 in Japanese pipistrelle: implications for the origin of the novel Middle East respiratory syndrome coronavirus. J Virol **87**:8638–8650. doi:10.1128/JVI.01055-13.
14. **Annan A, Baldwin HJ, Corman VM, Klose SM, Owusu M, Nkrumah EE, Badu EK, Anti P, Agbenyega O, Meyer B, Oppong S, Sarkodie YA, Kalko, Elisabeth K V, Lina, Peter H C, Godlevska EV, Reusken C, Seebens A, Gloza-Rausch F, Vallo P, Tschapka M, Drosten C, Drexler JF.** 2013. Human betacoronavirus 2c EMC/2012-related viruses in bats, Ghana and Europe. Emerging infectious diseases **19**:456–459. doi:10.3201/eid1903.121503.
15. **Corman VM, Ithete NL, Richards LR, Schoeman MC, Preiser W, Drosten C, Drexler JF.** 2014. Rooting the phylogenetic tree of middle East respiratory syndrome coronavirus by characterization of a conspecific virus from an African bat. J Virol **88**:11297–11303. doi:10.1128/JVI.01498-14.

16. **Peiris, J S M, Guan Y, Yuen KY.** 2004. Severe acute respiratory syndrome. Nat Med **10**:S88-97. doi:10.1038/nm1143.

17. **Bai B, Lu X, Meng J, Hu Q, Mao P, Lu B, Chen Z, Yuan Z, Wang H.** 2008. Vaccination of mice with recombinant baculovirus expressing spike or nucleocapsid protein of SARS-like coronavirus generates humoral and cellular immune responses. Molecular immunology **45**:868–875. doi:10.1016/j.molimm.2007.08.010.

18. **Du L, Zhao G, Chan, Chris C S, Sun S, Chen M, Liu Z, Guo H, He Y, Zhou Y, Zheng B, Jiang S.** 2009. Recombinant receptor-binding domain of SARS-CoV spike protein expressed in mammalian, insect and E. coli cells elicits potent neutralizing antibody and protective immunity. Virology **393**:144–150. doi:10.1016/j.virol.2009.07.018.

19. **Liniger M, Zuniga A, Tamin A, Azzouz-Morin TN, Knuchel M, Marty RR, Wiegand M, Weibel S, Kelvin D, Rota PA, Naim HY.** 2008. Induction of neutralising antibodies and cellular immune responses against SARS coronavirus by recombinant measles viruses. Vaccine **26**:2164–2174. doi:10.1016/j.vaccine.2008.01.057.

20. **Dimitrov DS.** 2004. Virus entry: molecular mechanisms and biomedical applications. Nature reviews. Microbiology **2**:109–122. doi:10.1038/nrmicro817.

21. **Hofmann H, Pöhlmann S.** 2004. Cellular entry of the SARS coronavirus. Trends in microbiology **12**:466–472. doi:10.1016/j.tim.2004.08.008.

22. **Song F, Fux R, Provacia LB, Volz A, Eickmann M, Becker S, Osterhaus, Albert D M E, Haagmans BL, Sutter G.** 2013. Middle East respiratory syndrome coronavirus spike protein delivered by modified vaccinia virus Ankara efficiently induces virus-neutralizing antibodies. J Virol **87**:11950–11954. doi:10.1128/JVI.01672-13.

23. **Kim E, Okada K, Kenniston T, Raj VS, AlHajri MM, Farag, Elmoubasher A B A, AlHajri F, Osterhaus, Albert D M E, Haagmans BL, Gambotto A.** 2014. Immunogenicity of an adenoviral-based Middle East Respiratory Syndrome coronavirus vaccine in BALB/c mice. Vaccine **32**:5975–5982. doi:10.1016/j.vaccine.2014.08.058.

24. **Gierer S, Bertram S, Kaup F, Wrensch F, Heurich A, Krämer-Kühl A, Welsch K, Winkler M, Meyer B, Drosten C, Dittmer U, Hahn T von, Simmons G, Hofmann H, Pöhlmann S.** 2013. The spike protein of the emerging betacoronavirus EMC uses a novel coronavirus receptor for entry, can be activated by TMPRSS2, and is targeted by neutralizing antibodies. J Virol **87**:5502–5511. doi:10.1128/JVI.00128-13.

25. **Raj VS, Mou H, Smits SL, Dekkers, Dick H W, Müller MA, Dijkman R, Muth D, Demmers, Jeroen A A, Zaki A, Fouchier, Ron A M, Thiel V, Drosten C, Rottier, Peter J M, Osterhaus, Albert D M E, Bosch BJ, Haagmans BL.** 2013. Dipeptidyl peptidase 4 is a functional receptor for the emerging human coronavirus-EMC. Nature **495**:251–254. doi:10.1038/nature12005.

26. **He Y, Lu H, Siddiqui P, Zhou Y, Jiang S.** 2005. Receptor-binding domain of severe acute respiratory syndrome coronavirus spike protein contains multiple conformation-dependent epitopes that induce highly potent neutralizing antibodies. J Immunol **174**:4908–4915.

27. **Ma C, Li Y, Wang L, Zhao G, Tao X, Tseng CK, Zhou Y, Du L, Jiang S.** 2014. Intranasal vaccination with recombinant receptor-binding domain of MERS-CoV spike protein induces much stronger local mucosal immune responses than subcutaneous immunization: Implication for designing novel mucosal MERS vaccines. Vaccine **32**:2100–2108. doi:10.1016/j.vaccine.2014.02.004.

28. **Du L, Kou Z, Ma C, Tao X, Wang L, Zhao G, Chen Y, Yu F, Tseng CK, Zhou Y, Jiang S.** 2013. A truncated receptor-binding domain of MERS-CoV spike protein potently inhibits MERS-CoV infection and induces strong neutralizing antibody responses: implication for developing therapeutics and vaccines. PloS one **8**:e81587. doi:10.1371/journal.pone.0081587.

29. **Du L, Zhao G, Kou Z, Ma C, Sun S, Poon, Vincent K M, Lu L, Wang L, Debnath AK, Zheng B, Zhou Y, Jiang S.** 2013. Identification of a receptor-binding domain in the S protein of the novel human coronavirus Middle East respiratory syndrome coronavirus as an essential target for vaccine development. J Virol **87**:9939–9942. doi:10.1128/JVI.01048-13.

30. **Mou H, Raj VS, van Kuppeveld, Frank J M, Rottier, Peter J M, Haagmans BL, Bosch BJ.** 2013. The receptor binding domain of the new Middle East respiratory syndrome coronavirus maps to a 231-residue region in the spike protein that efficiently elicits neutralizing antibodies. J Virol **87**:9379–9383. doi:10.1128/JVI.01277-13.

31. **Lan J, Deng Y, Chen H, Lu G, Wang W, Guo X, Lu Z, Gao GF, Tan W.** 2014. Tailoring Subunit Vaccine Immunity with Adjuvant Combinations and Delivery Routes Using the Middle East Respiratory Coronavirus (MERS-CoV) Receptor-Binding Domain as an Antigen. PloS one **9**:e112602. doi:10.1371/journal.pone.0112602.

32. **Yang Z, Kong W, Huang Y, Roberts A, Murphy BR, Subbarao K, Nabel GJ.** 2004. A DNA vaccine induces SARS coronavirus neutralization and protective immunity in mice. Nature **428**:561–564. doi:10.1038/nature02463.

33. **Hilleman MR.** 2001. Current overview of the pathogenesis and prophylaxis of measles with focus on practical implications. Vaccine **20**:651–665.

34. **Griffin DE.** 2002. Measles Virus. *In* , Wiley Encyclopedia of Molecular Medicine. John Wiley & Sons, Inc. John Wiley & Sons, Inc, Hoboken, NJ, USA.

35. **F Radecke, P Spielhofer, H Schneider, K Kaelin, M Huber, C Dötsch, G Christiansen, and M A Billeter.** 1995. Rescue of measles viruses from cloned DNA. The Embo Journal **14**:5773–5784.

36. **Billeter MA, Naim HY, Udem SA.** 2009. Reverse genetics of measles virus and resulting multivalent recombinant vaccines: applications of recombinant measles viruses. Curr Top Microbiol Immunol **329**:129–162.

37. **Duprex WP, Rima BK.** 2002. Using green fluorescent protein to monitor measles virus cell-to-cell spread by time-lapse confocal microscopy. Methods in molecular biology (Clifton, N.J.) **183**:297–307. doi:10.1385/1-59259-280-5:297.

38. **Singh M, Billeter MA.** 1999. A recombinant measles virus expressing biologically active human interleukin-12. J Gen Virol **80 (Pt 1)**:101–106.

39. **Singh M, Cattaneo R, Billeter MA.** 1999. A recombinant measles virus expressing hepatitis B virus surface antigen induces humoral immune responses in genetically modified mice. J Virol **73**:4823–4828.

40. **Reyes-del Valle J, de la Fuente, Cynthia, Turner MA, Springfeld C, Apte-Sengupta S, Frenzke ME, Forest A, Whidby J, Marcotrigiano J, Rice CM, Cattaneo R.** 2012. Broadly Neutralizing Immune Responses against Hepatitis C Virus Induced by Vectored Measles Viruses and a Recombinant Envelope Protein Booster. J Virol **86**:11558–11566. doi:10.1128/JVI.01776-12.

41. **Lorin C, Mollet L, Delebecque F, Combredet C, Hurtrel B, Charneau P, Brahic M, Tangy F.** 2004. A Single Injection of Recombinant Measles Virus Vaccines Expressing Human Immunodeficiency Virus (HIV) Type 1 Clade B Envelope Glycoproteins Induces Neutralizing Antibodies and Cellular Immune Responses to HIV. J Virol **78**:146–157. doi:10.1128/JVI.78.1.146-157.2004.

42. **Desprès P, Combredet C, Frenkiel M, Lorin C, Brahic M, Tangy F.** 2005. Live measles vaccine expressing the secreted form of the West Nile virus envelope glycoprotein protects against West Nile virus encephalitis. The Journal of infectious diseases **191**:207–214. doi:10.1086/426824.

43. **Brandler S, Marianneau P, Loth P, Lacôte S, Combredet C, Frenkiel M, Desprès P, Contamin H, Tangy F.** 2012. Measles vaccine expressing the secreted form of West Nile virus envelope glycoprotein induces protective immunity in squirrel monkeys, a new model of West Nile virus infection. The Journal of infectious diseases **206**:212–219. doi:10.1093/infdis/jis328.

44. **Brandler S, Ruffie C, Najburg V, Frenkiel M, Bedouelle H, Desprès P, Tangy F.** 2010. Pediatric measles vaccine expressing a dengue tetravalent antigen elicits neutralizing antibodies against all four dengue viruses. Vaccine **28**:6730–6739. doi:10.1016/j.vaccine.2010.07.073.

45. **Brandler S, Ruffié C, Combredet C, Brault J, Najburg V, Prevost M, Habel A, Tauber E, Desprès P, Tangy F.** 2013. A recombinant measles vaccine expressing chikungunya virus-like particles is strongly immunogenic and protects mice from lethal challenge with chikungunya virus. Vaccine **31**:3718–3725. doi:10.1016/j.vaccine.2013.05.086.

46. **Mrkic B, Pavlovic J, Rülicke T, Volpe P, Buchholz CJ, Hourcade D, Atkinson JP, Aguzzi A, Cattaneo R.** 1998. Measles Virus Spread and Pathogenesis in Genetically Modified Mice. J Virol **72**:7420–7427.

47. **Ramsauer K, Schwameis M, Firbas C, Müllner M, Putnak RJ, Thomas SJ, Desprès P, Tauber E, Jilma B, Tangy F.** 2015. Immunogenicity, safety, and tolerability of a recombinant measles-virus-based chikungunya vaccine: a randomised, double-blind, placebo-controlled, active-comparator, first-in-man trial. The Lancet. Infectious diseases **15**:519–527. doi:10.1016/S1473-3099(15)70043-5.

48. **del Valle, Jorge Reyes, Devaux P, Hodge G, Wegner NJ, McChesney MB, Cattaneo R.** 2007. A vectored measles virus induces hepatitis B surface antigen antibodies while protecting macaques against measles virus challenge. J Virol **81**:10597–10605. doi:10.1128/JVI.00923-07.

49. **Bajenoff M, Germain RN.** 2009. B-cell follicle development remodels the conduit system and allows soluble antigen delivery to follicular dendritic cells. Blood **114**:4989–4997. doi:10.1182/blood-2009-06-229567.

50. **Pape KA, Catron DM, Itano AA, Jenkins MK.** 2007. The humoral immune response is initiated in lymph nodes by B cells that acquire soluble antigen directly in the follicles. Immunity **26**:491–502. doi:10.1016/j.immuni.2007.02.011.

51. **Becker G de, Moulin V, Tielemans F, Mattia F de, Urbain J, Leo O, Moser M.** 1998. Regulation of T helper cell differentiation in vivo by soluble and membrane proteins provided by antigen-presenting cells. Eur J Immunol **28**:3161–3171. doi:10.1002/(SICI)1521-4141(199810)28:10<3161:AID-IMMU3161>3.0.CO;2-Q.

52. **Enriquez-Rincon F, Klaus GG.** 1984. Differing effects of monoclonal anti-hapten antibodies on humoral responses to soluble or particulate antigens. Immunology **52**:129–136.

53. **Shen Z, Reznikoff G, Dranoff G, Rock KL.** 1997. Cloned dendritic cells can present exogenous antigens on both MHC class I and class II molecules. J Immunol **158**:2723–2730.

54. **Martin A, Staeheli P, Schneider U.** 2006. RNA polymerase II-controlled expression of antigenomic RNA enhances the rescue efficacies of two different members of the Mononegavirales independently of the site of viral genome replication. J Virol **80**:5708–5715. doi:10.1128/JVI.02389-05.

55. **Hewett JW, Tannous B, Niland BP, Nery FC, Zeng J, Li Y, Breakefield XO.** 2007. Mutant torsinA interferes with protein processing through the secretory pathway in DYT1 dystonia cells. Proc Natl Acad Sci U S A **104**:7271–7276. doi:10.1073/pnas.0701185104.

56. **Boussif O, Lezoualc'h F, Zanta MA, Mergny MD, Scherman D, Demeneix B, Behr JP.** 1995. A versatile vector for gene and oligonucleotide transfer into cells in culture and in vivo: polyethylenimine. Proc Natl Acad Sci U S A **92**:7297–7301.

57. **Zufferey R, Nagy D, Mandel RJ, Naldini L, Trono D.** 1997. Multiply attenuated lentiviral vector achieves efficient gene delivery in vivo. Nat Biotechnol **15**:871–875. doi:10.1038/nbt0997-871.

58. **Münch RC, Mühlebach MD, Schaser T, Kneissl S, Jost C, Plückthun A, Cichutek K, Buchholz CJ.** 2011. DARPins: an efficient targeting domain for lentiviral vectors. Molecular therapy : the journal of the American Society of Gene Therapy **19**:686–693. doi:10.1038/mt.2010.298.

59. **Bach P, Abel T, Hoffmann C, Gal Z, Braun G, Voelker I, Ball CR, Johnston, Ian C D, Lauer UM, Herold-Mende C, Mühlebach MD, Glimm H, Buchholz CJ.** 2013. Specific

937 elimination of CD133+ tumor cells with targeted oncolytic measles virus. Cancer research
938 **73**:865–874. doi:10.1158/0008-5472.CAN-12-2221.
939 60. **Kärber G.** 1931. Beitrag zur kollektiven Behandlung pharmakologischer Reihenversuche.
940 Archiv f. experiment. Pathol. u. Pharmakol **162**:480–483. doi:10.1007/BF01863914.
941 61. **Funke S, Maisner A, Mühlebach MD, Koehl U, Grez M, Cattaneo R, Cichutek K,**
942 **Buchholz CJ.** 2008. Targeted cell entry of lentiviral vectors. Molecular therapy : the journal
943 of the American Society of Gene Therapy **16**:1427–1436. doi:10.1038/mt.2008.128.
944 62. **Kuhn AN, Diken M, Kreiter S, Selmi A, Kowalska J, Jemielity J, Darzynkiewicz E,**
945 **Huber C, Tureci O, Sahin U.** 2010. Phosphorothioate cap analogs increase stability and
946 translational efficiency of RNA vaccines in immature dendritic cells and induce superior
947 immune responses in vivo. Gene Ther **17**:961–971. doi:10.1038/gt.2010.52.
948 63. **Kreiter S, Konrad T, Sester M, Huber C, Tureci O, Sahin U.** 2007. Simultaneous ex vivo
949 quantification of antigen-specific CD4+ and CD8+ T cell responses using in vitro
950 transcribed RNA. Cancer Immunol Immunother **56**:1577–1587. doi:10.1007/s00262-007-
951 0302-7.
952 64. **Lyons AB, Parish CR.** 1994. Determination of lymphocyte division by flow cytometry.
953 Journal of immunological methods **171**:131–137.
954 65. **Corman VM, Eckerle I, Bleicker T, Zaki A, Landt O, Eschbach-Bludau M, van**
955 **Boheemen S, Gopal R, Ballhause M, Bestebroer TM, Muth D, Muller MA, Drexler JF,**
956 **Zambon M, Osterhaus AD, Fouchier RM, Drosten C.** 2012. Detection of a novel human
957 coronavirus by real-time reverse-transcription polymerase chain reaction. Euro Surveill **17**.
958 66. **Coleman CM, Matthews KL, Goicochea L, Frieman MB.** 2014. Wild-type and innate
959 immune-deficient mice are not susceptible to the Middle East respiratory syndrome
960 coronavirus. J Gen Virol **95**:408–412. doi:10.1099/vir.0.060640-0.
961 67. **Coleman CM, Liu YV, Mu H, Taylor JK, Massare M, Flyer DC, Glenn GM, Smith GE,**
962 **Frieman MB.** 2014. Purified coronavirus spike protein nanoparticles induce coronavirus
963 neutralizing antibodies in mice. Vaccine **32**:3169–3174. doi:10.1016/j.vaccine.2014.04.016.
964 68. **Ma C, Wang L, Tao X, Zhang N, Yang Y, Tseng CK, Li F, Zhou Y, Jiang S, Du L.**
965 2014. Searching for an ideal vaccine candidate among different MERS coronavirus receptor-
966 binding fragments--the importance of immunofocusing in subunit vaccine design. Vaccine
967 **32**:6170–6176. doi:10.1016/j.vaccine.2014.08.086.

69. **Dhiman N, Jacobson RM, Poland GA.** 2004. Measles virus receptors: SLAM and CD46. Reviews in medical virology **14**:217–229. doi:10.1002/rmv.430.

70. **Mühlebach MD, Mateo M, Sinn PL, Prüfer S, Uhlig KM, Leonard, Vincent H. J., Navaratnarajah CK, Frenzke M, Wong XX, Sawatsky B, Ramachandran S, McCray PB, Cichutek K, Messling V von, Lopez M, Cattaneo R**. Adherens junction protein nectin-4 (PVRL4) is the epithelial receptor for measles virus. Nature **480**:530–533. doi:10.1038/nature10639.

71. **Maeyer E de, Enders JF.** 1961. An Interferon Appearing in Cell Cultures Infected with Measles Virus. Experimental Biology and Medicine **107**:573–578. doi:10.3181/00379727-107-26692.

72. **Leopardi R, Hyypiä T, Vainionpää R.** 1992. Effect of interferon-alpha on measles virus replication in human peripheral blood mononuclear cells. APMIS : acta pathologica, microbiologica, et immunologica Scandinavica **100**:125–131.

73. **Mills CD, Kincaid K, Alt JM, Heilman MJ, Hill AM.** 2000. M-1/M-2 Macrophages and the Th1/Th2 Paradigm. The Journal of Immunology **164**:6166–6173. doi:10.4049/jimmunol.164.12.6166.

74. **Scott P.** 1993. Selective differentiation of CD4+ T helper cell subsets. Current Opinion in Immunology **5**:391–397. doi:10.1016/0952-7915(93)90058-Z.

75. **Brenner GJ, Cohen N, Moynihan JA.** 1994. Similar immune response to nonlethal infection with herpes simplex virus-1 in sensitive (BALB/c) and resistant (C57BL/6) strains of mice. Cellular immunology **157**:510–524. doi:10.1006/cimm.1994.1246.

76. **Chow, Ken Y C, Yeung YS, Hon CC, Zeng F, Law KM, Leung, Frederick C C.** 2005. Adenovirus-mediated expression of the C-terminal domain of SARS-CoV spike protein is sufficient to induce apoptosis in Vero E6 cells. FEBS letters **579**:6699–6704. doi:10.1016/j.febslet.2005.10.065.

77. **Yeung Y, Yip C, Hon C, Chow, Ken Y C, Ma, Iris C M, Zeng F, Leung, Frederick C C.** 2008. Transcriptional profiling of Vero E6 cells over-expressing SARS-CoV S2 subunit: insights on viral regulation of apoptosis and proliferation. Virology **371**:32–43. doi:10.1016/j.virol.2007.09.016.

78. **Liu R, Wu L, Huang B, Huang J, Zhang Y, Ke M, Wang J, Tan W, Zhang R, Chen H, Zeng Y, Huang W.** 2005. Adenoviral expression of a truncated S1 subunit of SARS-CoV

spike protein results in specific humoral immune responses against SARS-CoV in rats. Virus research **112**:24–31. doi:10.1016/j.virusres.2005.02.009.

79. **Weingartl H, Czub M, Czub S, Neufeld J, Marszal P, Gren J, Smith G, Jones S, Proulx R, Deschambault Y, Grudeski E, Andonov A, He R, Li Y, Copps J, Grolla A, Dick D, Berry J, Ganske S, Manning L, Cao J.** 2004. Immunization with modified vaccinia virus Ankara-based recombinant vaccine against severe acute respiratory syndrome is associated with enhanced hepatitis in ferrets. J Virol **78**:12672–12676. doi:10.1128/JVI.78.22.12672-12676.2004.

80. **Czub M, Weingartl H, Czub S, He R, Cao J.** 2005. Evaluation of modified vaccinia virus Ankara based recombinant SARS vaccine in ferrets. Vaccine **23**:2273–2279. doi:10.1016/j.vaccine.2005.01.033.

81. **An S, Chen CJ, Yu X, Leibowitz JL, Makino S.** 1999. Induction of apoptosis in murine coronavirus-infected cultured cells and demonstration of E protein as an apoptosis inducer. J Virol **73**:7853–7859.

82. **Subbarao K, McAuliffe J, Vogel L, Fahle G, Fischer S, Tatti K, Packard M, Shieh W, Zaki S, Murphy B.** 2004. Prior infection and passive transfer of neutralizing antibody prevent replication of severe acute respiratory syndrome coronavirus in the respiratory tract of mice. J Virol **78**:3572–3577.

83. **Seo SH, Wang L, Smith R, Collisson EW.** 1997. The carboxyl-terminal 120-residue polypeptide of infectious bronchitis virus nucleocapsid induces cytotoxic T lymphocytes and protects chickens from acute infection. J Virol **71**:7889–7894.

84. **Yu L, Liu W, Schnitzlein WM, Tripathy DN, Kwang J.** 2001. Study of protection by recombinant fowl poxvirus expressing C-terminal nucleocapsid protein of infectious bronchitis virus against challenge. Avian Dis **45**:340–348.

85. **Du L, Zhao G, Lin Y, Sui H, Chan C, Ma S, He Y, Jiang S, Wu C, Yuen K, Jin D, Zhou Y, Zheng B.** 2008. Intranasal vaccination of recombinant adeno-associated virus encoding receptor-binding domain of severe acute respiratory syndrome coronavirus (SARS-CoV) spike protein induces strong mucosal immune responses and provides long-term protection against SARS-CoV infection. J Immunol **180**:948–956.

86. **Agrawal AS, Garron T, Tao X, Peng B, Wakamiya M, Chan T, Couch RB, Tseng CK.** 2015. Generation of Transgenic Mouse Model of Middle East Respiratory Syndrome-Coronavirus Infection and Disease. J Virol. doi:10.1128/JVI.03427-14.

87. **Tangy F, Naim HY.** 2005. Live attenuated measles vaccine as a potential multivalent pediatric vaccination vector. Viral immunology **18**:317–326. doi:10.1089/vim.2005.18.317.

88. **Garbutt M, Liebscher R, Wahl-Jensen V, Jones S, Moller P, Wagner R, Volchkov V, Klenk H, Feldmann H, Stroher U.** 2004. Properties of replication-competent vesicular stomatitis virus vectors expressing glycoproteins of filoviruses and arenaviruses. J Virol **78**:5458–5465.

89. **Jones SM, Feldmann H, Stroher U, Geisbert JB, Fernando L, Grolla A, Klenk H, Sullivan NJ, Volchkov VE, Fritz EA, Daddario KM, Hensley LE, Jahrling PB, Geisbert TW.** 2005. Live attenuated recombinant vaccine protects nonhuman primates against Ebola and Marburg viruses. Nat Med **11**:786–790. doi:10.1038/nm1258.

90. **WHO**. http://www.who.int/mediacentre/news/statements/2014/second-ebola-vaccine/en/.

Figure Legends

Fig.1. Generation and characterization of MV_{vac2}-MERS-S and MV_{vac2}-MERS-solS. (A) Schematic depiction of full-length MERS-S and a soluble variant lacking the transmembrane and cytoplasmatic region (MERS-solS) (upper schemes) and recombinant MV_{vac2} genomes used for expression of those (lower schemes). Antigen or antigen encoding genes are depicted in dark grey; MV viral gene cassettes (in light grey) are annotated. *MluI* and *AatII* restriction sites used for cloning of antigen-genes into post P or post H ATU are highlighted (B) Immunoblot analysis of Vero cells infected at an MOI of 0.03 with MV_{vac2}-MERS-S, MV_{vac2}-MERS-solS, or MV_{vac2}-GFP(H) (MV_{vac2}) as depicted above lanes. Uninfected cells served as mock. Blots were probed using rabbit serum reactive against MERS-CoV (upper blot) or mAb reactive against MV-N (lower blot). Arrows indicate specific bands. (C, D) Growth kinetics of recombinant MV on Vero cells infected at an MOI of 0.02 with MV_{vac2}-MERS-S (MERS-S), MV_{vac2}-MERS-solS (MERS-solS), or MV_{vac2}-GFP encoding extra genes in post H (C) or post P (D) ATU. Titers of samples prepared at indicated time points post infection were titrated on Vero cells. Means and standard deviations of three independent experiments are presented. ns, not significant.

1058

1059 **Fig.2. Induction of antibodies specifically binding MERS-S or MV antigens**. Sera of mice
1060 vaccinated on days 0 and 28 with indicated viruses were sampled on days -7 (pre-bleed, A) and
1061 49 (B) and analyzed for antibodies binding MERS-S or MV bulk antigens by ELISA. Medium-
1062 inoculated mice served as mock control. Antibodies binding to recombinant MERS-S or MV bulk
1063 antigens are detectable by OD_{405} in the ELISA. Means and standard deviation of each group are
1064 depicted (n = 6; filled triangles, MV_{vac2}-MERS-S(H); filled circles, MV_{vac2}-MERS-solS(H); open
1065 circles, mock; open squares, MV_{vac2}-ATU(P)).

1066

1067 **Fig.3. Analysis of neutralizing antibodies.** Virus neutralizing titers (VNT) of animals
1068 vaccinated on days 0 and 28 with indicated viruses sampled on day -7 (A,D), 28 (B,E), and 49
1069 (C,F) completely neutralizing 200 $TCID_{50}$ of MERS-CoV or 50 pfu of MV. Medium-inoculated
1070 mice served as mock. VNT were calculated as reciprocal of the highest dilution abolishing
1071 infectivity. Dots represent single animals (n = 10); horizontal line represents mean per group. Y-
1072 axis starts at detection limit; all mice at detection limit had no detectable VNT. ns, not
1073 significant; *, P<0,05; **, P<0,01; *** P<0,0001

1074

1075 **Fig.4. Secretion of IFN-γ after antigen-specific restimulation of splenocytes.** IFN-γ ELISpot
1076 analysis using splenocytes of mice vaccinated on days 0 and 28 with indicated viruses, isolated 4
1077 d after boost immunization, and after co-culture with JAWSII (A), DC2.4 (B), or DC3.2 (C)
1078 dendritic cell lines transgenic for MERS-S (black columns) or untransduced controls (white
1079 columns). (D) To analyse cellular responses directed against MV, splenocytes were stimulated
1080 with 10 µg/ml MV bulk antigens (grey columns) or left unstimulated (white columns). The
1081 reactivity of splenocytes was confirmed by ConA treatment (10 µg/ml) (speckled columns).

Presented are means and standard deviation per group (n = 6). ns, not significant; *, $P < 0.05$; **, $P < 0.01$.

Fig.5. Induction of MERS-S specific CTLs. (A) Proliferation assay using splenocytes of mice vaccinated on days 0 and 28 with MV_{vac2}-MERS-S(H) or MV_{vac2}-MERS-solS(H), isolated 21 d after boost immunization, and after co-culture with JAWSII dendritic cell lines transgenic for MERS-S (right, filled triangles) or untransduced controls (left, filled circles). Depicted are the percentages of $CD8^+$ T cells with low CFSE indicating proliferation in the samples. Results for splenocytes of vaccinated mice are displayed individually and trend between paired unstimulated and re-stimulated samples is outlined. Splenocytes of control vaccinated mice (open circles, mock; open squares, MV_{vac2}-ATU(P)) were pooled. (B, C) Killing assay using splenocytes of mice vaccinated on days 0 and 28 isolated 4 d after boost immunization. Splenocytes were co-cultured with untransduced JAWSII (B) or with antigen-presenting JAWSII-MERS-S (C) or for 6 days. Activated CTLs were then co-cultured with EL-4-MERS-S target cells (Antigen) and EL-4_{red} control cells (N) at indicated E:T ratios for 4 h. Ratio of living target to non-target cells (Antigen:NC) was determined by flow cytometry. Depicted (filled triangles, MV_{vac2}-MERS-S(H); filled circles, MV_{vac2}-MERS-solS(H); open circles, mock; open squares, MV_{vac2}-ATU(P)) are means and standard deviation of each group (n = 6). ns, not significant; *, $P < 0.05$; **, $P < 0.01$; *** $P < 0.0001$

Fig.6 Viral load after MERS-CoV challenge *in vivo*. (A, B) Viral load determined as (A) genome copies per ng RNA or (B) infectious virus titers in the lungs of pre-vaccinated mice after transduction with DPP4-encoding AdV 21 d after boost, and challenge with MERS-CoV 25 day after boost. 2 independent experiments with n = 4-5 per group. Error bars, SEM; dotted line,

LOD (LOD of qPCR < 1.7 copies/ng RNA); ns, not significant; *, P < 0.05 (C) AdV transduction control, mCherry mRNA copies per ng RNA. Error bars, SEM.

Fig.7 Histopathological changes and immunohistochemical analysis of lungs after challenge. Analysis of lung tissue of representative pre-vaccinated mice (as indicated) after transduction with hDPP4-encoding AdV and challenge with MERS-CoV. Pictures arranged in one row were from samples of the same individual mouse. Paraffin-fixed tissue was stained with hematoxylin and eosin (H&E, first column; scale bar 200 µm), with Ab against MERS-CoVspike antigen (middle column; scale bar 100 µm), and as control of AdV transduction against mCherry (left column; scale bar 50 µm).

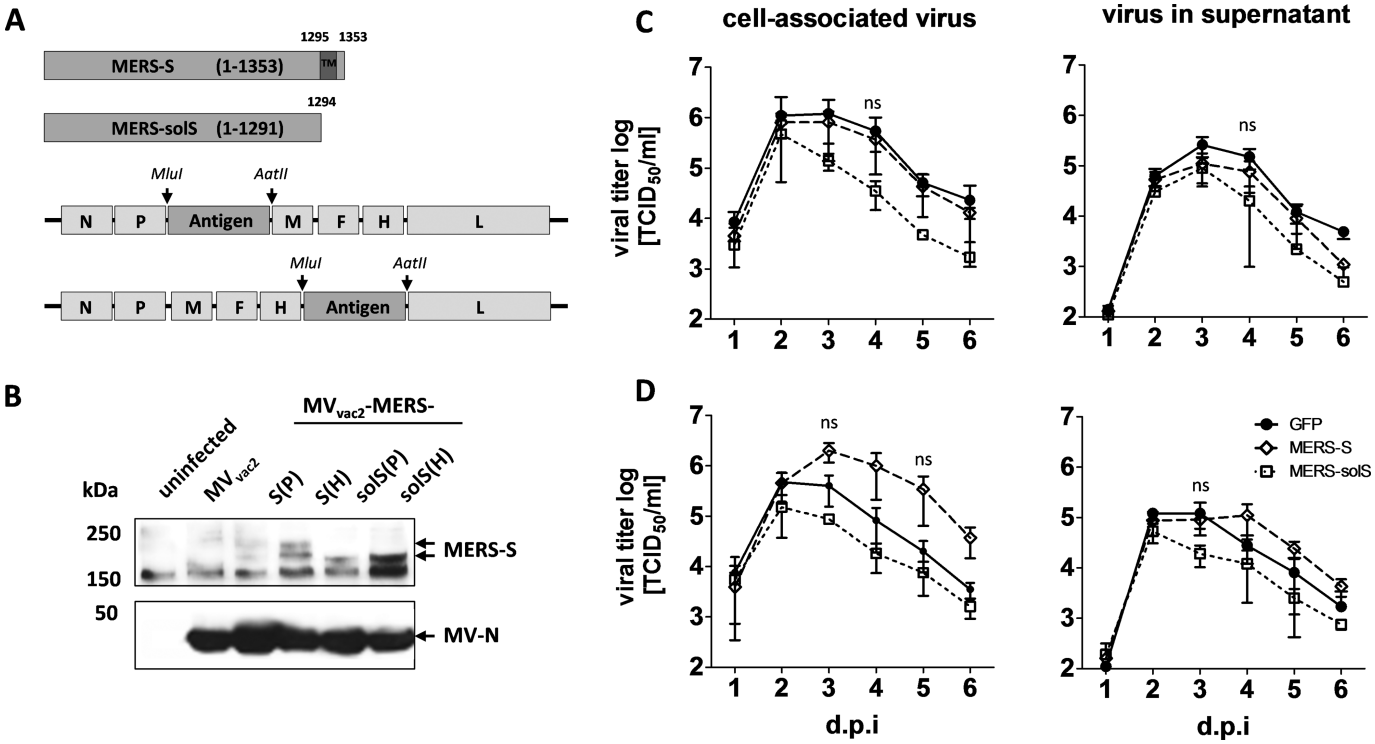

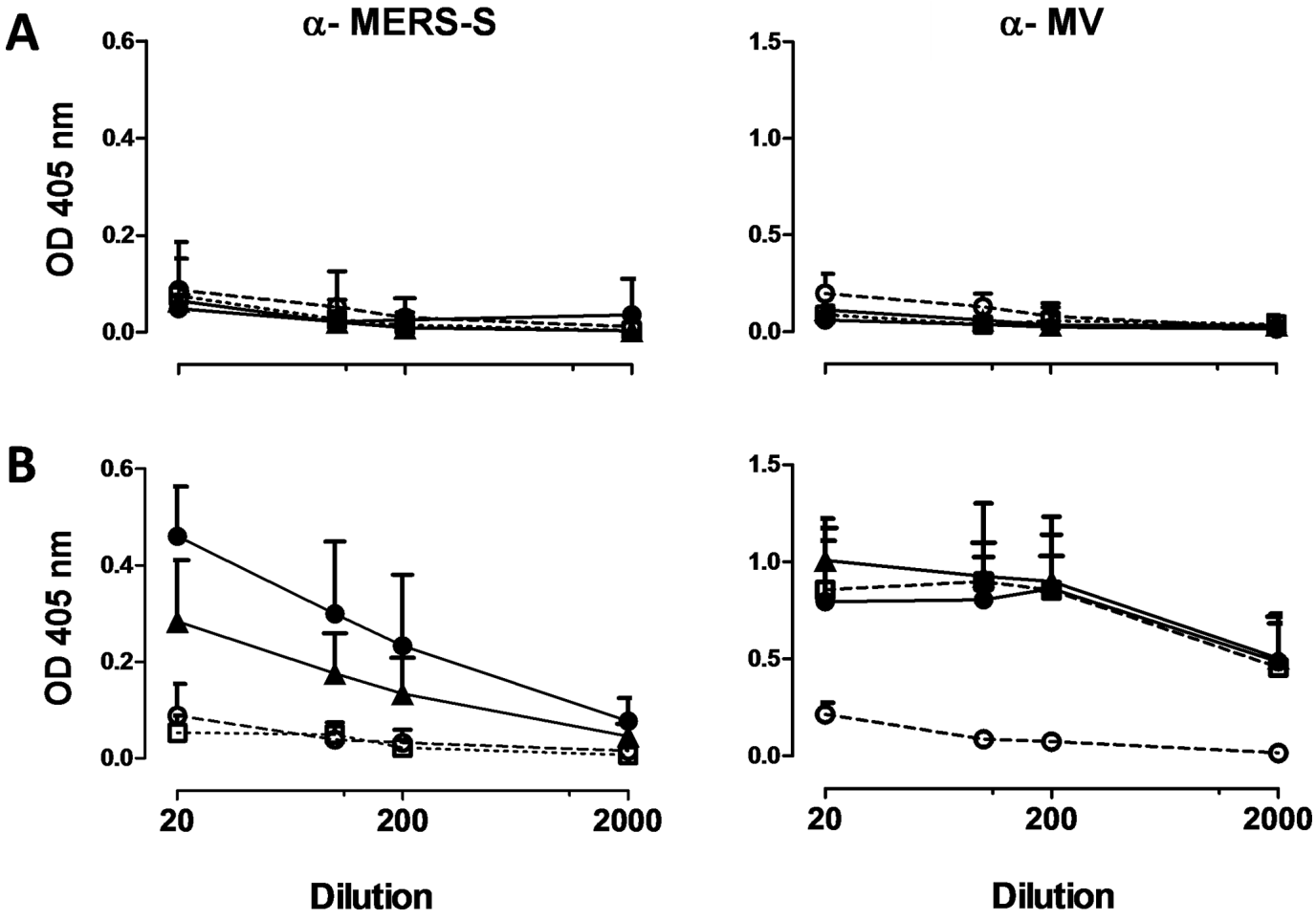

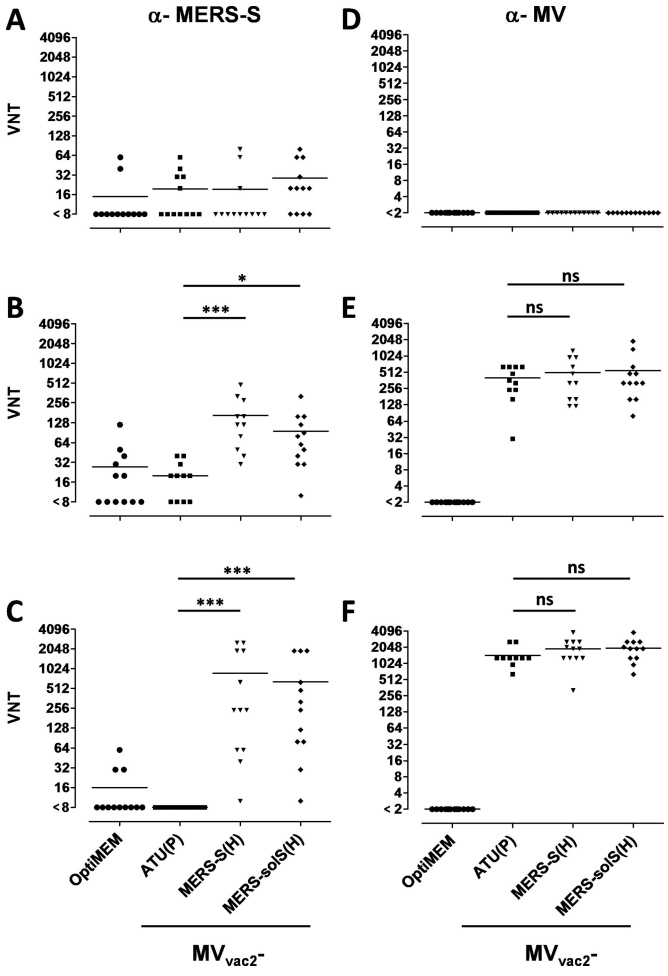

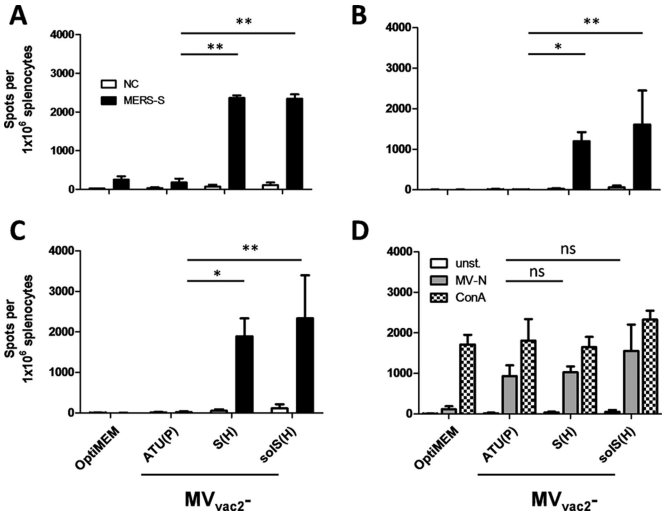

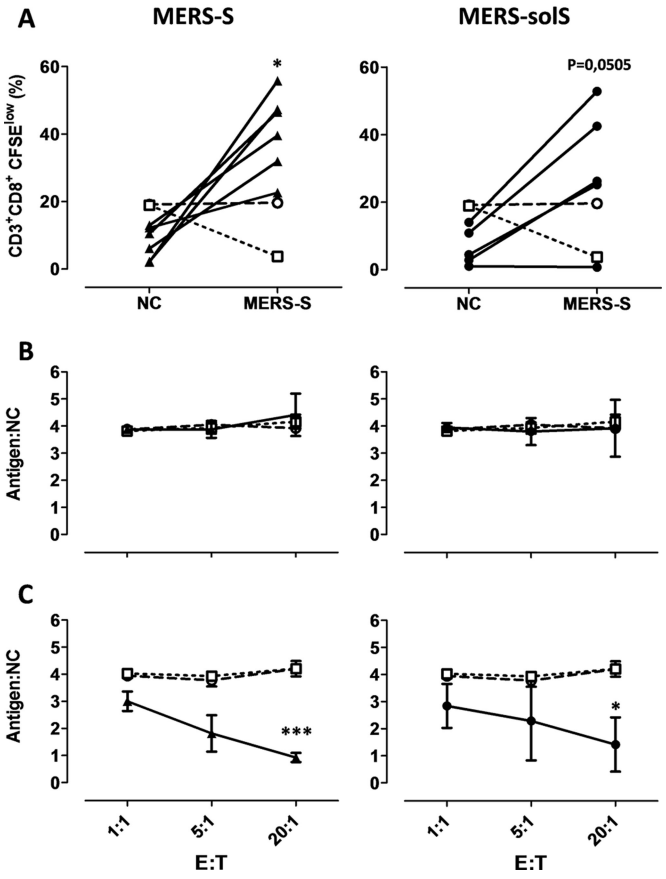

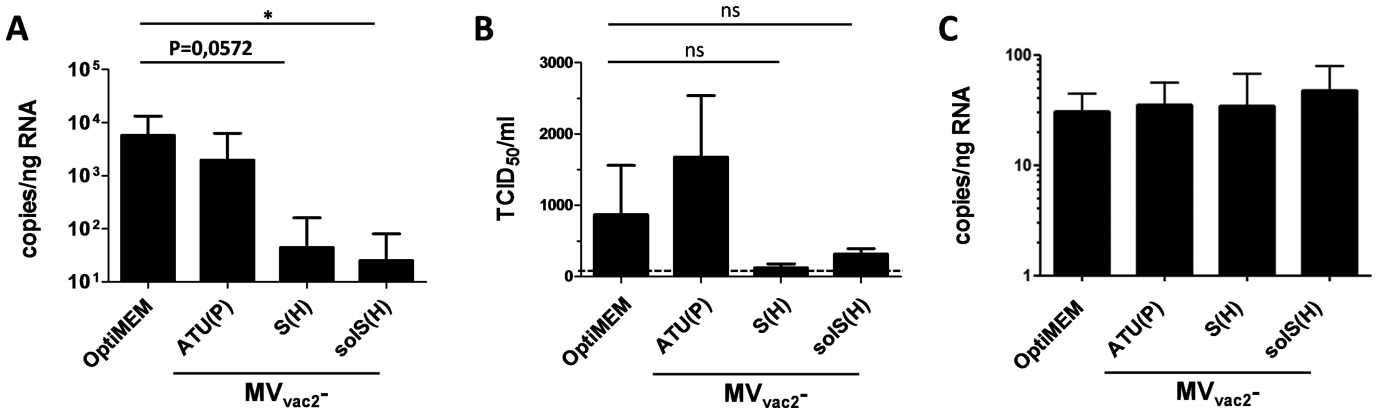

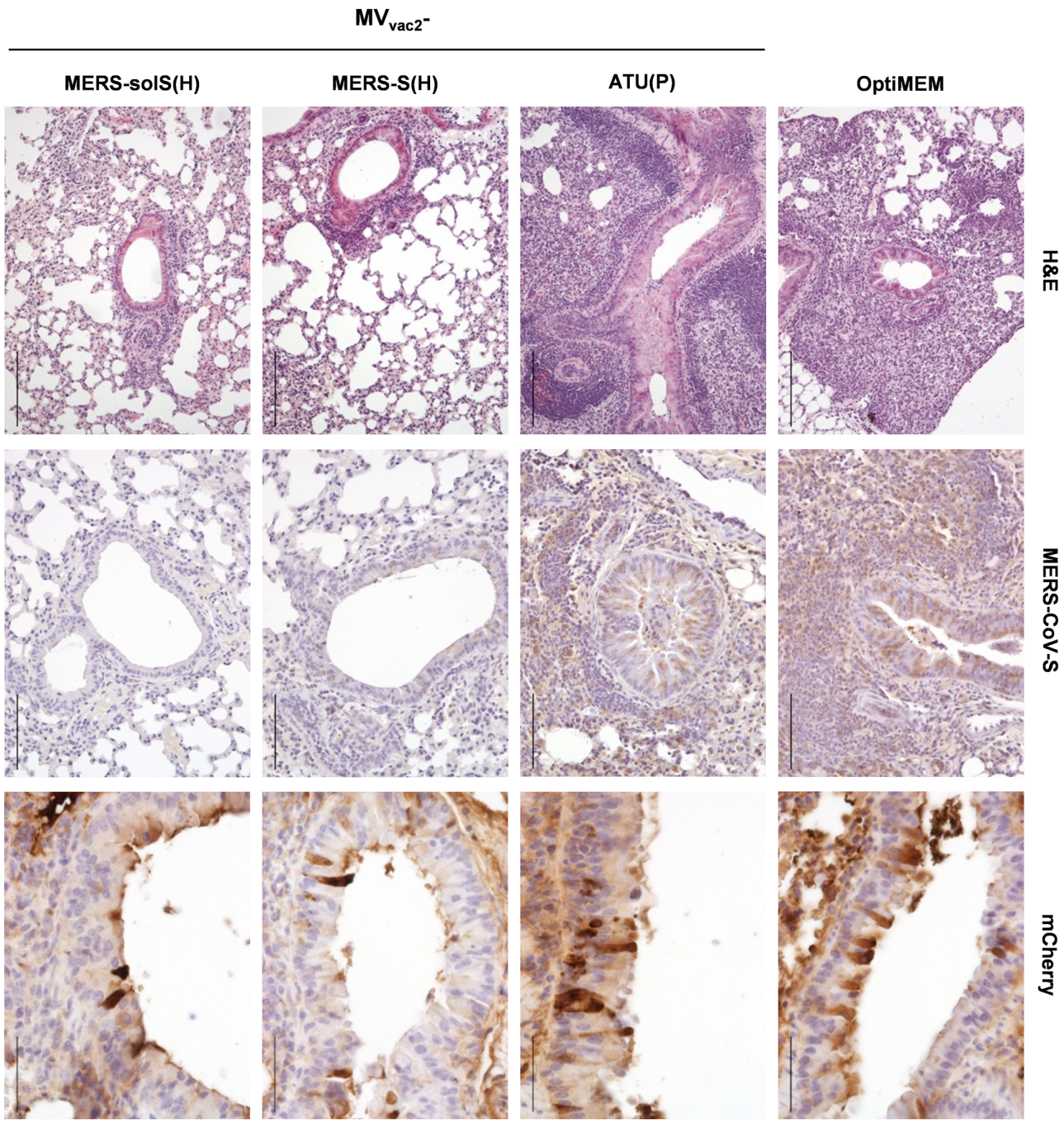
MV$_{vac2}$-
MERS-solS(H)
MERS-S(H)
ATU(P)
OptiMEM
H&E
MERS-CoV-S
mCherry